CHAPTER 38

CRYOGENICS

CRYOGENICS is a term normally associated with low temperatures. However, the location on the temperature scale at which refrigeration generally ends and cryogenics begins has never been well defined. Most scientists and engineers working in this field restrict cryogenics to a temperature below −235°F (225°R), because the normal boiling points of most permanent gases (e.g., helium, hydrogen, neon, nitrogen, argon, oxygen, and air) occur below this temperature. In contrast, most common refrigerants have boiling points above this temperature.

Cryogenic engineering therefore is involved with the design and development of low-temperature systems and components. In such activities the designer must be familiar with the properties of fluids used to achieve these low temperatures as well as the physical properties of components used to produce, maintain, and apply such temperatures.

GENERAL APPLICATIONS

The application of cryogenic engineering has become extensive. In the United States, for example, nearly 30% of the oxygen produced by cryogenic separation is used by the steel industry to reduce the cost of high-grade steel, and another 20% is used in the chemical process industry to produce a variety of oxygenated compounds. Liquid hydrogen production has risen from laboratory quantities to over 200 tons/day. Similarly, liquid helium demand has required the construction of large plants to separate helium from natural gas cryogenically. Energy demand likewise has accelerated construction of large base-load liquefied natural gas (LNG) plants. Applications include high-field magnets and sophisticated electronic devices that use the superconductivity of materials at low temperatures. Space simulation requires cryopumping (freezing residual gases in a chamber on a cold surface) to provide the ultrahigh vacuum representative of conditions in space. This concept has also been used in commercial high-vacuum pumps.

The food industry uses large amounts of liquid nitrogen to freeze expensive foods such as shrimp and to maintain frozen food during transport. Liquid-nitrogen-cooled containers are used to preserve whole blood, bone marrow, and animal semen for extended periods. Cryogenic surgery is performed to treat disorders such as Parkinson’s disease. Medical diagnosis uses magnetic resonance imaging (MRI), which requires cryogenically cooled superconducting magnets. Superconducting magnets are now an essential component in high-energy accelerators and target chambers. Finally, the chemical processing industry relies on cryogenic temperatures to recover valuable heavy components or upgrade the heat content of fuel gas from natural gas, recover useful components such as argon and neon from air, purify various process and waste streams, and produce ethylene from a mixture of olefin compounds.

LOW-TEMPERATURE PROPERTIES

Test data are necessary because properties at low temperatures are often significantly different from those at ambient temperatures. For example, the onset of ductile-to-brittle transitions in carbon steel, the phenomenon of superconductivity, and the vanishing of specific heats cannot be inferred from property measurements obtained at ambient temperatures.

Fluid Properties

Some thermodynamic data for cryogenic fluids are given in Chapter 20 of the 2005 *ASHRAE Handbook—Fundamentals*. Computer-compiled tabulations include those of MIPROPS prepared by NIST; GASPAK, HEPAK, and PROMIX developed by Cryodata (Arp 1998); and EES [Klein (continuously updated)]. Some key properties for selected cryogens are summarized in Table 1, including the normal boiling point (i.e., boiling point at atmospheric pressure), critical point, and triple point (nominally equal to the freezing point at atmospheric pressure). Table 1 also presents the volumetric enthalpy change associated with evaporation at atmospheric pressure, and the volumetric enthalpy change associated with heating saturated vapor at atmospheric pressure to room temperature. These quantities reflect the value of the cryogen in the conventional situation (where only the latent heat of evaporation is used) and the less typical situation where the sensible heat is also recovered.

Several cryogens have unique properties, discussed in the following sections.

Helium. Helium exists in two isotopic forms, the more common being helium 4. The rarer form, helium 3, exhibits a much lower vapor pressure, which has been exploited in the development of the helium dilution refrigerator to attain temperatures as low as 0.03 to 0.09°R. Whenever helium is referenced without isotopic designation, it can be assumed to be helium 4.

As a liquid, helium exhibits two unique phases: liquid helium I and liquid helium II (Figure 1). Helium I is labeled as the normal fluid and helium II as the superfluid because, under certain conditions, the fluid exhibits no viscosity. The phase transition between these two liquids is identified as the lambda (λ) line. Intersection of helium II with the vapor pressure curve is known as the λ point. Immediately to the right of the λ line, the specific heat of helium I increases to a large but finite value as the temperature approaches this line; therefore, although there is no specific volume change or latent heat associated with the helium I to II transition, a significant energy change is required. Once below the λ line, the specific heat of helium II rapidly decreases to zero. Figure 2 illustrates the specific heat capacity of helium at low temperatures, both above and below the λ line, and various pressures (data from HEPAK). Notice the sharp rise in specific heat capacity near –455.76°F (the λ line) at all pressures (essentially independent of pressure). Also note the specific heat fluctuations at higher temperatures, related to the normal two-phase behavior of a substance near its critical point.

The thermal conductivity of helium I decreases with decreasing temperature. However, once the transition to helium II has been

---

This preparation of this chapter is assigned to TC 10.4, Ultralow-Temperature Systems and Cryogenics.

Table 1 Key Properties of Selected Cryogens

Cryogen	Normal Boiling Temperature, °R	Critical Temperature, °R	Triple-Point Temperature, °R	Density of Saturated Liquid at 1 atm, lb$_m$/ft^3	Density of Saturated Vapor at 1 atm, lb$_m$/ft^3	Volumetric Enthalpy of Vaporization at 1 atm, Btu/ft^3*	Volumetric Enthalpy to Warm Vapor to 537°R at 1 atm, Btu/ft^3*
Helium	7.61	9.35	—	7.787	1.046	69.4	5212
Hydrogen	36.70	59.74	25.12	4.420	0.0836	845.5	4005
Neon	48.79	80.09	44.21	75.35	0.5979	2774	7476
Oxygen	162.34	278.25	97.85	71.24	0.2789	6535	8707
Nitrogen	139.24	227.15	113.67	50.32	0.2879	4303	6370
Argon	157.14	271.24	150.85	87.11	0.3604	6035	7629
Methane	201.00	343.02	163.25	26.37	0.1134	5790	7125

*Per cubic foot of saturated liquid cryogen at 1 atm.

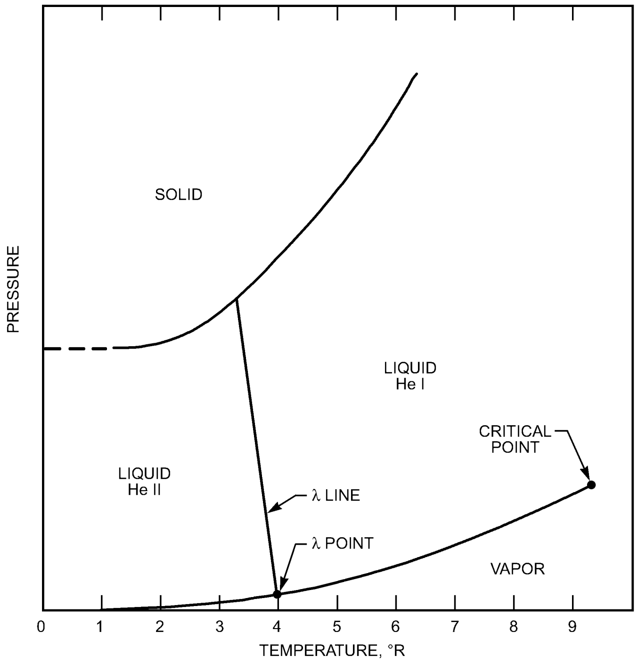

Fig. 1 Phase Diagram for Helium 4

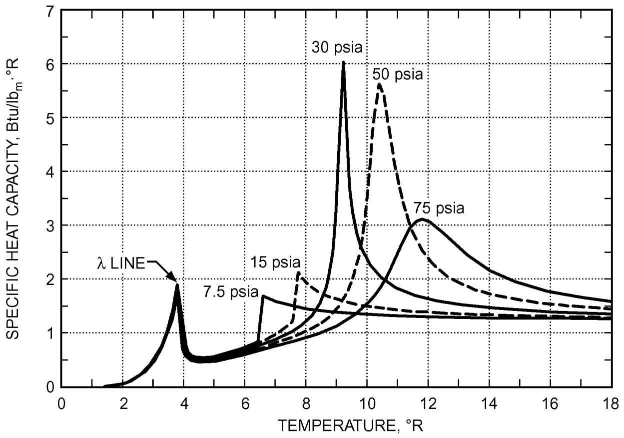

Fig. 2 Specific Heat for Helium 4 as Function of Temperature for Various Pressures

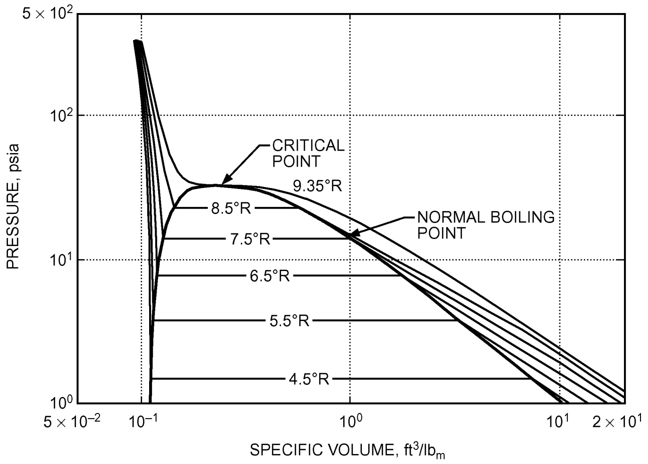

Fig. 3 Pressure/Volume Diagram for Helium 4 near Its Vapor Dome

made, the thermal conductivity of the liquid has no real physical meaning, yet the heat transfer characteristics of helium II are spectacular. As the vapor pressure above helium I is reduced, the fluid boils vigorously. As the liquid pressure decreases, its temperature also decreases as the liquid boils away. When the temperature reaches the λ point and the helium transitions to helium II, all bubbling suddenly stops. The liquid becomes clear and quiet, although it is still vaporizing quite rapidly at the surface. The apparent thermal conductivity of helium II is so large that vapor bubbles do not have time to form within the body of the fluid before the heat is conducted to the surface of the liquid. Liquid helium I has a thermal conductivity of approximately 0.0139 Btu/h·ft·°R, whereas liquid helium II can have an apparent thermal conductivity as large as 49,112 Btu/h·ft·°R, approximately six orders of magnitude larger. This characteristic makes He II the ideal coolant for low-temperature applications, including superconducting magnets (Barron 1985). Also, helium 4 has no triple point and requires a pressure of 360 psia or more to exist as a solid below a temperature of −455°F (5°R).

Figure 3 illustrates the pressure/volume diagram of helium 4 near its vapor dome, and clearly shows the critical point and normal boiling point. Note that the density of the liquid and vapor phases of liquid helium far from the critical point differ only by a factor of about 7.5, compared to 1000 for many substances. Also, the latent heat of vaporization for helium is only 9 Btu/lb (or 70 Btu/ft^3 of liquid helium), which is very small; thus, the amount of heat that can be absorbed by a bath of liquid helium is limited, so liquid nitrogen shielding is needed, as well as stringent requirements for thermal isolation. Notice that the amount of energy that can be absorbed by evaporation of liquid helium if the sensible heat capacity of the vapor is included is far larger: 5260 Btu/lb^3 (Table 1). Therefore, the flow of the helium vapor as it warms to room temperature is often controlled to ensure that this sensible heat is properly used.

Hydrogen. A distinctive property of hydrogen is that it can exist in two molecular forms: orthohydrogen and parahydrogen. These forms differ by having parallel (orthohydrogen) or opposed (parahydrogen) nuclear spins associated with the two atoms forming the hydrogen molecule. At ambient temperatures, the equilibrium mixture of 75% orthohydrogen and 25% parahydrogen is designated as normal hydrogen. With decreasing temperatures, the thermodynamics shift to 99.79% parahydrogen at –423°F (36.7°R), the normal boiling point of hydrogen. Conversion from normal hydrogen to parahydrogen is exothermic and evolves sufficient energy to vaporize ~1% of the stored liquid per hour, assuming negligible heat leak into the storage container. The fractional rate of conversion is given by

$$\frac{dx}{d\theta} = -kx^2 \tag{1}$$

where x is the orthohydrogen fraction at time θ in hours and k is the reaction rate constant, 0.0114/h. The fraction of liquid remaining in a storage dewar at time θ is then

$$\ln\frac{m}{m_o} = \frac{1.57}{1.33 + 0.0114\theta} - 1.18 \tag{2}$$

Here m_o is the mass of normal hydrogen at $\theta = 0$ and m is the mass of remaining liquid at time θ. If the original composition of the liquid is not normal hydrogen at $\theta = 0$, a new constant of integration based on the initial orthohydrogen concentration can be evaluated from Equation (1). Figure 4 summaries the calculations.

To minimize such losses in commercial production of liquid hydrogen, a catalyst is used to hasten the conversion from normal hydrogen to the thermodynamic equilibrium concentration during liquefaction. Hydrous iron oxide, Cr_2O_3 on an Al_2O_3 gel carrier, or NiO on an Al_2O_3 gel are used as catalysts. The latter combination is about 90 times as rapid as the others and is therefore the preferred choice.

Figure 5 shows a pressure/volume diagram for hydrogen.

Oxygen. Unlike other cryogenic fluids, liquid oxygen (LOX) is slightly magnetic. Its paramagnetic susceptibility is 1.003 at its normal boiling point. This characteristic has prompted the use of a magnetic field in a liquid oxygen dewar to separate the liquid and gaseous phases under zero-gravity conditions.

Both gaseous and liquid oxygen are chemically reactive, particularly with hydrocarbon materials. Because oxygen presents a serious safety problem, systems using liquid oxygen must be maintained scrupulously clean of any foreign matter. Liquid oxygen cleanliness in the space industry has come to be associated with a set of elaborate cleaning and inspection specifications representing a near ultimate in large-scale equipment cleanliness.

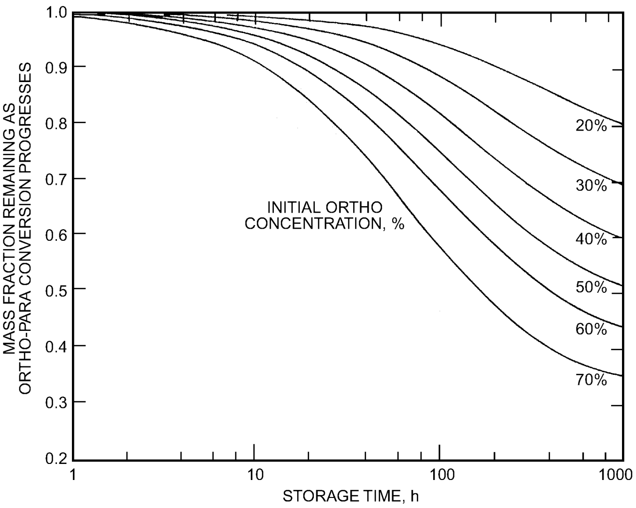

Fig. 4 Fraction of Liquid Hydrogen Evaporated due to Ortho-Parahydrogen Conversion as Function of Storage Time

Nitrogen. Liquid nitrogen (LIN) is of considerable importance as a cryogen because it is a safe refrigerant. Because it is rather inactive chemically and is neither explosive nor toxic, liquid nitrogen is commonly used in hydrogen and helium liquefaction cycles as a precoolant. Figure 6 illustrates the pressure/volume diagram for nitrogen near its vapor dome.

Liquefied Natural Gas (LNG). Liquefied natural gas is the liquid form of natural gas, consisting primarily of methane, a mixture of heavier hydrocarbons, and other impurities such as nitrogen and hydrogen sulfide. Liquefying natural gas reduces its specific volume by a factor of approximately 600 to 1, which makes handling and storage economically possible despite the added cost of liquefaction and the need for insulated transport and storage equipment.

Thermal Properties

Specific heat, thermal conductivity, and thermal expansivity are of major interest at low temperatures.

Specific Heat. Specific heat can be predicted fairly accurately by mathematical models through statistical mechanics and quantum theory. For solids, the Debye model gives a satisfactory representation of

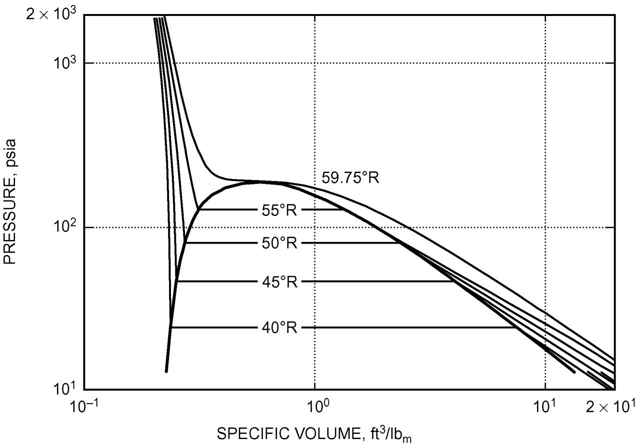

Fig. 5 Pressure/Volume Diagram for Hydrogen near Its Vapor Dome

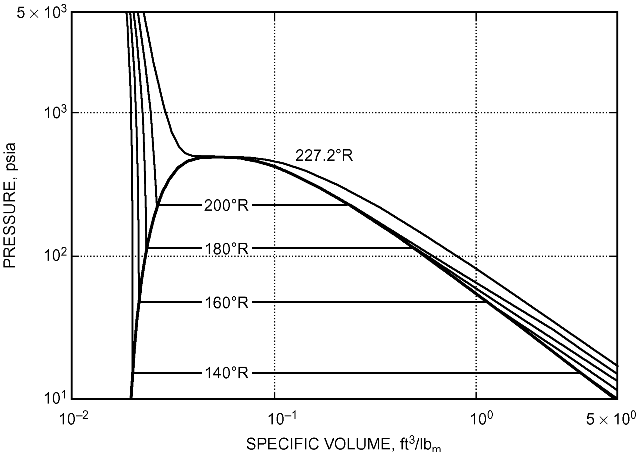

Fig. 6 Pressure/Volume Diagram for Nitrogen near Its Vapor Dome

specific heat with changes in temperature. However, difficulties are encountered when applying the Debye theory to alloys and compounds.

Several computer programs provide thermal data for many metals used in low-temperature equipment. METALPAK (Arp 1997), for example, is a reference program for the thermal properties of 13 metals used in low-temperature systems.

The specific heat of cryogenic liquids generally decreases in a manner similar to that observed for crystalline solids as the temperature is lowered. At low pressures, specific heat decreases with a decrease in temperature. However, at high pressures near the critical point, humps appear in the specific heat curve for all cryogenic fluids.

Figure 7 illustrates the specific heat capacity of several commonly used solid materials as a function of temperature. In general, specific heat decreases with decreasing temperature.

Often, the specific heat must be known to determine the amount of energy to remove from a material to cool it from room temperature (80.3°F) to cryogenic temperatures. The integrated average specific heat $\bar{c}$ is useful for this type of calculation:

$$\bar{c}(T) = \frac{1}{(T_{room} - T)} \int_{T}^{T_{room}} c(T)\,dT \tag{3}$$

Figure 8 illustrates the integrated average (from room temperature) specific heat for various solid materials.

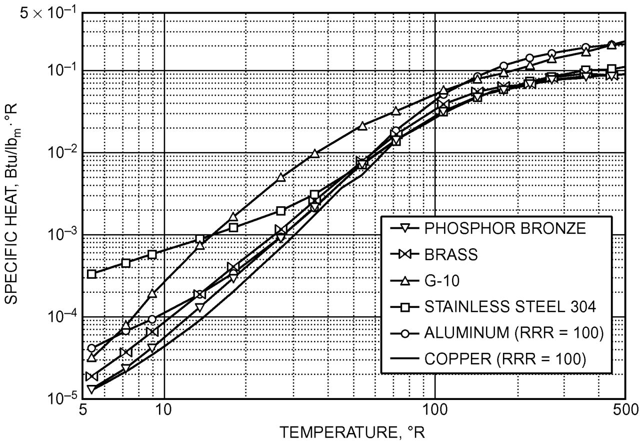

Fig. 7 Specific Heat of Common Cryogenic Materials

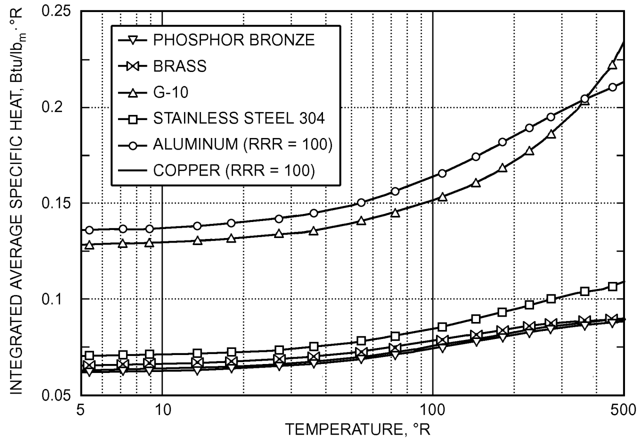

Fig. 8 Integrated Average Specific Heat (from 540°R) for Common Cryogenic Materials

Table 2 summarizes the integrated average specific heat for various materials and for several temperature ranges.

Thermal Conductivity. Thermal conductivity of pure metals at low temperatures can be accurately predicted with the Wiedeman-Franz law, which states that the ratio of thermal conductivity to the product of the electrical conductivity and absolute temperature is a constant. This ratio for high-conductivity metals extrapolates close to the Sommerfeld value of 2.58×10^{-8} Btu·Ω/(h·°R^2) at absolute zero, but is considerably below this value at higher temperatures. However, high-purity aluminum and copper peak in thermal conductivity between 423 and –370°F (36 and 90°R), but these peaks are rapidly suppressed with increased impurity levels or cold work of the metal. Aluminum alloys, for example, steadily decrease in thermal conductivity as temperature decreases. Other structural alloys, such as those of nickel-copper (67% Ni/30% Cu), nickel-chromium-iron (78% Ni/16% Cr/6% Fe), and stainless steel, exhibit similar thermal conductivity properties and thus are helpful in reducing heat leak into a cryogenic system.

Figure 9 illustrates the thermal conductivity of some common cryogenic materials. Note that the thermal conductivity of copper and other metals is extremely sensitive to the purity of the material below about –350°F. The purity of copper is often reported using the residual resistance ratio (RRR) value, which is the ratio of the electrical resistivity of the material at room temperature to its resistivity at –452°F. An RRR value of 100 is typical for commercial-grade copper.

Often, the thermal conductivity is needed to determine the conduction heat leak associated with a structure made of the material between room temperature (80.3°F) and some cryogenic temperatures. The integrated average thermal conductivity $\bar{k}$ is useful for this type of calculation:

$$\bar{k}(T) = \frac{1}{(T_{room} - T)} \int_{T}^{T_{room}} k(T)\,dT \tag{4}$$

Figure 10 illustrates the integrated average (from room temperature) thermal conductivity for various solid materials. Table 3

Table 2 Integrated Average Specific Heat for Cryogenic Materials, in Btu/lb$_m$·°R

	540 to 270°R	540 to 150°R	540 to 35°R	540 to 7°R
Copper (RRR = 100)	0.0866	0.0800	0.0673	0.0639
Aluminum (RRR = 100)	0.196	0.176	0.145	0.137
304 stainless steel	0.100	0.0906	0.0755	0.0716
G-10	0.186	0.1620	0.135	0.129
Brass	0.0882	0.0825	0.0702	0.0666
Phosphor bronze	0.0850	0.0785	0.0663	0.0629

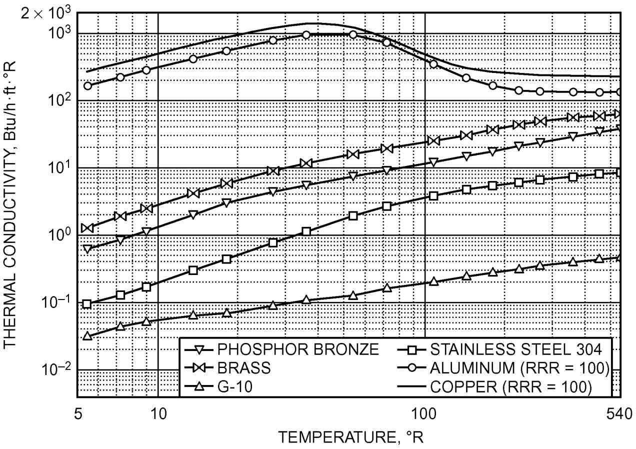

Fig. 9 Thermal Conductivity of Common Cryogenic Materials

summarizes the integrated average thermal conductivity for various materials and for several temperature ranges.

Thermal Expansion Coefficient. The expansion coefficient of a solid can be estimated with an approximate thermodynamic equation of state for solids that equates the volumetric thermal expansion coefficient with the quantity $\gamma c_v \rho / B$, where γ is the Grüneisen dimensionless ratio, c_v the specific heat of the solid, ρ the density of the material, and B its bulk modulus. For face-centered cubic metals, the average value of the Grüneisen constant is approximately 2.3. However, this constant tends to increase with atomic number. Figure 11 illustrates the integrated average coefficient of thermal expansion $\bar{\alpha}$ from room temperature, defined as

$$\bar{\alpha}(T) = \frac{1}{(T_{room} - T)} \int_{T}^{T_{room}} \alpha(T)\,dT \qquad (5)$$

Electrical and Magnetic Properties

The ratio of the electrical resistivity of most pure metallic elements at ambient temperature to that at moderately low temperatures is approximately proportional to the ratio of the absolute temperatures. However, at very low temperatures, the electrical resistivity (except of superconductors) approaches a residual value almost independent of temperature. Alloys, on the other hand, have resistivities much higher than those of their constituent elements and exhibit very low resistance temperature coefficients. Electrical resistivity is thus largely independent of temperature and may often be of the same magnitude as the ambient temperature value.

The insulating quality of solid electrical conductors usually improves with decreased temperature. However, from 2 to 10°R, the electrical resistivity of many semiconductors increases quite rapidly with a small decrease in temperature. This has formed the basis for the development of numerous sensitive semiconductor resistance thermometers for very-low-temperature measurements. Figure 12 illustrates the electrical resistivity of several common cryogenic materials.

Table 3 Integrated Average Thermal Conductivity for Cryogenic Materials, in Btu/h·ft·°F

Material	80.3 to –190°F	80.3 to –316°F	80.3 to –424°F	80.3 to –452°F
Copper (RRR = 100)	2806	2902	4135	4544
Aluminum (RRR = 100)	1627	1711	2798	3045
304 Stainless steel	93.60	85.98	75.57	72.11
G-10	5.061	4.645	4.091	3.952
Brass	693.3	630.3	551.9	526.9
Phosphor bronze	380.6	334.2	291.9	276.6

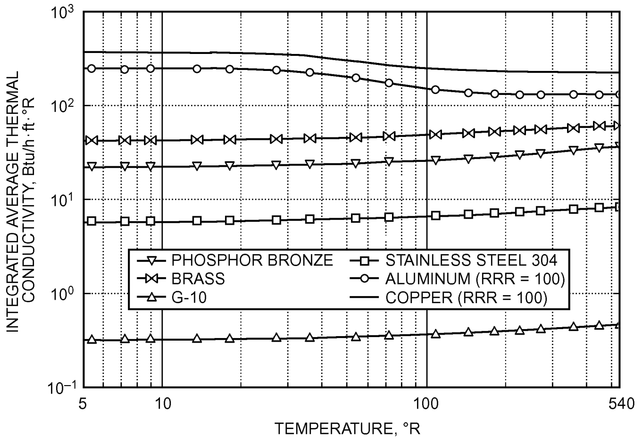

Fig. 10 Integrated Average Thermal Conductivity (from 540°R) for Common Cryogenic Materials

Superconductivity. Superconductivity is described as the disappearance of electrical resistance in certain materials that are maintained below a characteristic temperature, electrical current, and magnetic field, and the appearance of perfect diamagnetism, which is the most distinguishing characteristic of superconductors.

More than 26 elements have been shown to be superconductors at low temperatures at ambient pressure, and at least 10 more at higher pressure. In fact, the number of materials with identified superconducting properties extends into the thousands. Bednorz and Müller's (1986) discovery of high-temperature superconductors and the intensive research to extend the upper temperature limit above 243°R have further increased this list of superconductors.

For all superconductors, the superconducting state is defined by the region below three interdependent critical parameters: temperature, current density, and magnetic field. At zero field and current density, the critical temperature for all elemental superconductors is below 18°R; for low-temperature alloys, it is below 45°R; and for the high-temperature compounds, it extends up to 243°R. Critical current densities of practical interest for magnet and electronics applications range from 1000 to 50,000 A/mm^2 for fields less than 50,000 gauss, and fall to zero, depending on the superconductor, between 90,000 and 280,000 gauss. The BSCCO (bismuth, strontium,

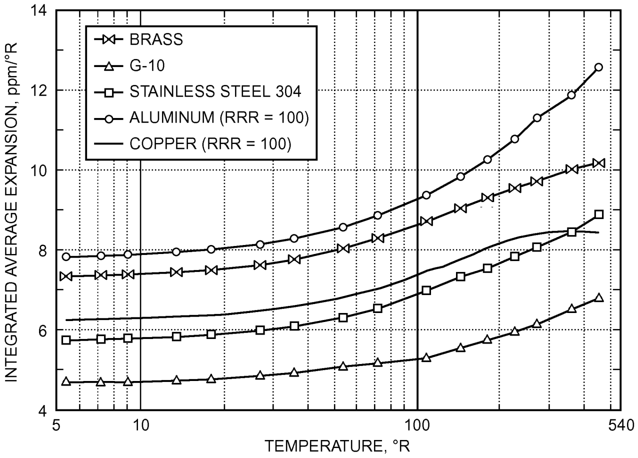

Fig. 11 Integrated Average Thermal Coefficient of Expansion (from 540°R) for Common Cryogenic Materials

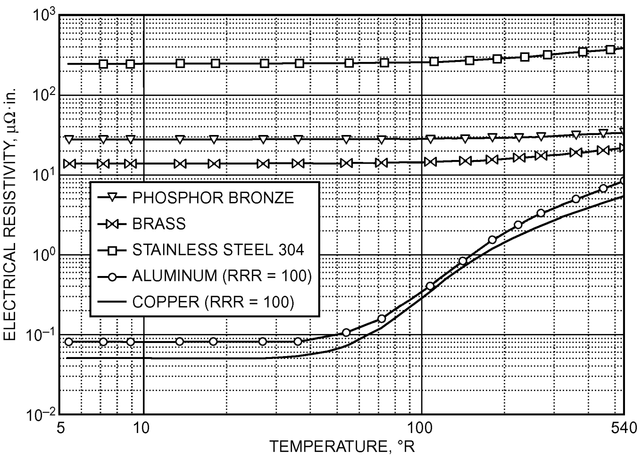

Fig. 12 Electrical Resistivity of Some Common Cryogenic Materials

(Data from Eckels Engineering)

copper, carbon, and oxygen) and YBCO (yttrium, barium, copper, and oxygen) superconductors display the highest critical magnetic fields (above 250,000 gauss).

Properties affected when a material becomes superconducting include specific heat, thermal conductivity, electrical resistance, magnetic permeability, and thermoelectric effect. Consequently, use of superconducting materials in construction of equipment subjected to operating temperatures below their critical temperatures needs to be evaluated carefully.

Thermal conductivities of superconducting materials are significantly lower than the same materials in their normal (or nonsuperconducting) state. For example, increasing the magnetic field around a sample of lead (Pb) from 0 to 1000 gauss at a constant temperature of 4.5°R, and thereby causing it to transition from the superconducting to normal state, increases thermal conductivity tenfold. This property is used for thermal switches in low-temperature technologies. The relatively low thermal conductivity of high-temperature superconductors (0.58 to 2.33 Btu/h·ft·°R) provide a convenient means to transfer current with minimal accompanying heat from –316°F (144°R) stages down to superconducting systems at –452.47°F (7.2°R).

Mechanical Properties

Mechanical properties of interest for the design of a facility subjected to low temperatures include ultimate strength, yield strength, fatigue strength, impact strength, hardness, ductility, and elastic moduli. Chapter 40 and Wigley (1971) include information on some of these properties.

Mechanical properties of metals at low temperature are classified most conveniently by their lattice symmetry. **Face-centered cubic (fcc)** metals and their alloys are most often used in constructing cryogenic equipment. Al, Cu, Ni, their alloys, and the austenitic stainless steels of the 18-8 type are fcc and do not exhibit an impact ductile-to-brittle transition at low temperatures. As a general rule, the mechanical properties of these metals improve as the temperature is reduced. The yield strength at –423°F (36°R) is considerably larger than at ambient temperature; Young's modulus is 5 to 20% larger at the lower temperature, and fatigue properties, except those of 2024 T4 aluminum, are improved at the lower temperature. Because annealing can affect both the ultimate and yield strengths, care must be exercised under these conditions.

Body-centered cubic (bcc) metals and alloys are normally undesirable for low-temperature construction. This class includes Fe, the martensitic steels (low-carbon and the 400 series of stainless steels), Mo, and Nb. If not brittle at room temperature, these materials exhibit a ductile-to-brittle transition at low temperatures. Hard working of some steels, in particular, can induce the austenite-to-martensite transition.

Hexagonal close-packed (hcp) metals exhibit mechanical properties between those of the fcc and bcc metals. For example, Zn undergoes a ductile-to-brittle transition, but Zr and pure Ti do not. The latter and its alloys, having an hcp structure, remain reasonably ductile at low temperatures and have been used for many applications where weight reduction and reduced heat leakage through the material have been important. However, small impurities of O, N, H, and C can have detrimental effects on the low-temperature ductility properties of Ti and its alloys.

Plastics increase in strength as temperature decreases, but this increase in strength is also accompanied by a rapid decrease in elongation in a tensile test and decrease in impact resistance. Nonstick fluorocarbon resins and glass-reinforced plastics retain appreciable impact resistance as temperature decreases. Glass-reinforced plastics also have high strength-to-weight and strength-to-thermal-conductivity ratios. All elastomers, on the other hand, become brittle at low temperatures. Nevertheless, many of these materials, including rubber, polyester film, and nylon, can be used for static seal gaskets if they are highly compressed at room temperature before cooling.

The strength of **glass** under constant loading also increases with decreased temperature. Because failure occurs at a lower stress when the glass surface contains surface defects, strength can be improved by tempering the surface.

REFRIGERATION AND LIQUEFACTION

A refrigeration or liquefaction process at cryogenic temperatures usually involves ambient compression of a suitable fluid with heat rejected to a coolant. The fluid's enthalpy and entropy decrease during compression and cooling, but increase at the cryogenic temperature where heat is absorbed. The temperature of the process fluid is usually reduced by heat exchange with a returning colder fluid and then followed with an expansion of the process fluid. This expansion may take place using either a throttling device approximating an isenthalpic expansion, with only a reduction in temperature, or a work-producing device approximating an isentropic expansion, in which both temperature and enthalpy decrease.

Normal commercial refrigeration generally uses a vapor compression process. Temperatures down to about –100°F (360°R) can be obtained by cascading vapor compression, in which refrigeration is obtained by liquid evaporation in each stage. Below this temperature, isenthalpic and isentropic expansion are generally used, either singly or in combination. With few exceptions, refrigerators using these methods also absorb heat by vaporization of liquid. If no suitable liquid exists to absorb the heat by evaporation over a temperature range, a cold gas must be available to absorb the heat. This is generally accomplished by using a work-producing expansion engine.

In a continuous refrigeration process, no refrigerant accumulates in any part of the system. This is in contrast with a liquefaction system, where liquid accumulates and is continuously withdrawn. Thus, in a liquefaction system, the total mass of returning cold gas that is warmed before compression is less than the mass of gas that is to be cooled, creating an imbalance of flow in the heat exchangers. In a refrigerator, the mass flow rates of the warm- and cold-gas streams in the heat exchangers are usually equal, unless a portion of the warm-gas flow is diverted through a work-producing expander. This condition of equal flow is usually called a **balanced flow condition** in the heat exchangers.

Isenthalpic Expansion

The thermodynamic process identified either as the simple **Linde-Hampson cycle** or the **Joule-Thomson cycle (J-T cycle)** is shown schematically in Figure 13A. In this cycle, the gaseous refrigerant is compressed isothermally at ambient temperature by rejecting heat to a coolant. The compressed refrigerant is then cooled in a heat exchanger, with the cold-gas stream returning to the compressor intake. Joule-Thomson cooling accompanying the expansion of gas exiting the heat exchanger further reduces the temperature of the refrigerant until, under steady-state conditions, a small fraction of the refrigerant is liquefied. For a refrigerator, the liquid fraction is vaporized by absorbing the heat Q that is to be removed, combined with the unliquefied fraction, and, after warming in the heat exchanger, returned to the compressor. Figure 13B shows the ideal process on a temperature-entropy diagram.

Applying the first law to this refrigeration cycle, assuming no heat leaks to the system as well as negligible kinetic and potential energy changes in the refrigeration fluid, the refrigeration effect per unit mass of refrigeration is simply the difference in enthalpies of streams 1 and 2 in Figure 13A. Thus, the coefficient of performance (COP) of the ideal J-T cycle is given by

$$\mathrm{COP} = \frac{Q}{W} = \frac{h_1 - h_2}{T_1(s_1 - s_2) - (h_1 - h_2)} \tag{6}$$

where Q is the refrigeration effect, W the work of compression, h_1 and s_1 are the specific enthalpy and entropy at point 1, and h_2 and s_2 the specific enthalpy and entropy at point 2 of Figure 13A.

For a liquefier, the liquefied portion is continuously withdrawn from the liquid reservoir and only the unliquefied portion of the fluid is warmed in the heat exchanger and returned to the compressor. The fraction y that is liquefied is determined by applying the first law to the heat exchanger, J-T valve, and liquid reservoir. This results in

$$y = \frac{h_1 - h_2}{h_1 - h_f} \tag{7}$$

where h_f is the specific enthalpy of the saturated liquid being withdrawn. The maximum liquefaction occurs when the difference between h_1 and h_2 is maximized.

To account for any heat leak Q_L into the system, Equation (7) needs to be modified to

$$y = \frac{h_1 - h_2 - Q_L}{h_1 - h_f} \tag{8}$$

resulting in a decrease in the fraction liquefied. The work of compression is identical to that determined for the J-T refrigerator. The figure of merit (FOM) is defined as $(W/m_f)_i/(W/m_f)$, where $(W/m_f)_i$ is the work of compression per unit mass liquefied for the ideal liquefier and (W/m_f) is the work of compression per unit mass liquefied for the J-T liquefier. The FOM reduces to

$$\text{FOM} = \left[\frac{T_1(s_1 - s_f) - (h_1 - h_f)}{T_1(s_1 - s_2) - (h_1 - h_2)}\right]\left(\frac{h_1 - h_2}{h_1 - h_f}\right) \tag{9}$$

Liquefaction by this cycle requires that the inversion temperature of the refrigerant be above ambient temperature. Auxiliary refrigeration is required if the J-T cycle is to be used to liquefy fluids with an inversion temperature below ambient (e.g., helium, hydrogen, neon). Liquid nitrogen is the optimum auxiliary refrigerant for hydrogen and neon liquefaction systems, and liquid hydrogen accompanied by liquid nitrogen are the normal auxiliary refrigerants for helium liquefaction systems. Upper operating pressures for the J-T cycle are often as high as 3000 psia.

To reduce the work of compression in the previous cycle, a two-stage or dual-pressure cycle may be used in which the pressure is reduced by two successive isenthalpic expansions, as shown in Figure 14. Because the work of compression is approximately proportional to the logarithm of the pressure ratio, and the Joule-Thomson cooling is roughly proportional to the pressure difference, compressor work is reduced by more than the refrigeration performance. Hence, the dual-pressure process produces the same quantity of refrigeration with less energy input than the simple J-T process.

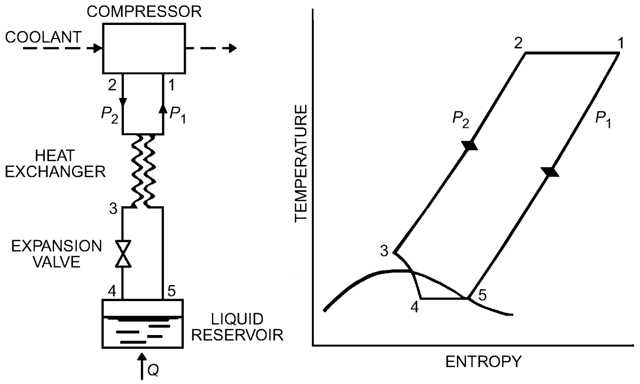

A. SCHEMATIC B. DIAGRAM

Fig. 13 Schematic and Temperature-Entropy Diagram for Simple Joule-Thomson Cycle Refrigerator

The theoretical liquid yield for the dual-pressure J-T cycle is obtained by making an energy balance around the cold heat exchanger, lower J-T valve, and liquid reservoir as follows:

$$(m - m_f - m_i)h_1 + m_i h_2 + m_f h_f - m h_3 = 0 \tag{10}$$

where m, m_f, and m_i are the mass flow rates of the streams designated in Figure 14. Solving for the liquid yield y for the ideal dual-pressure cycle gives

$$y = \frac{h_1 - h_3}{h_1 - h_f} - \frac{m_i}{m}\left(\frac{h_1 - h_2}{h_1 - h_f}\right) \tag{11}$$

The intermediate pressure in this cycle must be optimized. For a cycle with an upper pressure of 3000 psia, the intermediate optimum pressure generally occurs between 580 and 1015 psia.

Isentropic Expansion

Because temperature always decreases in a work-producing expansion, cooling does not depend on being below the inversion temperature before expansion. In large industrial refrigerators, work produced during the expansion is conserved with an expansion turbine. In small refrigerators, energy from expansion is usually dissipated in a gas or hydraulic pump or other suitable device.

A schematic of a refrigerator using the work-producing expansion principle and the corresponding temperature-entropy diagram are shown in Figure 15. Gas compressed isothermally at ambient temperature is cooled in a heat exchanger by gas being warmed on its return to the compressor intake. Further cooling takes place in the expansion engine. In practice, this expansion is never truly isentropic, as shown by path 3-4 on the temperature-entropy diagram. The refrigerator shown produces a cold gas that absorbs heat during path 4-5 and provides a method of refrigeration that can be used to obtain temperatures between those of the boiling points of the lower-boiling cryogenic fluids.

The coefficient of performance of an ideal gas refrigerator with varying refrigerator temperature can be obtained from the relation

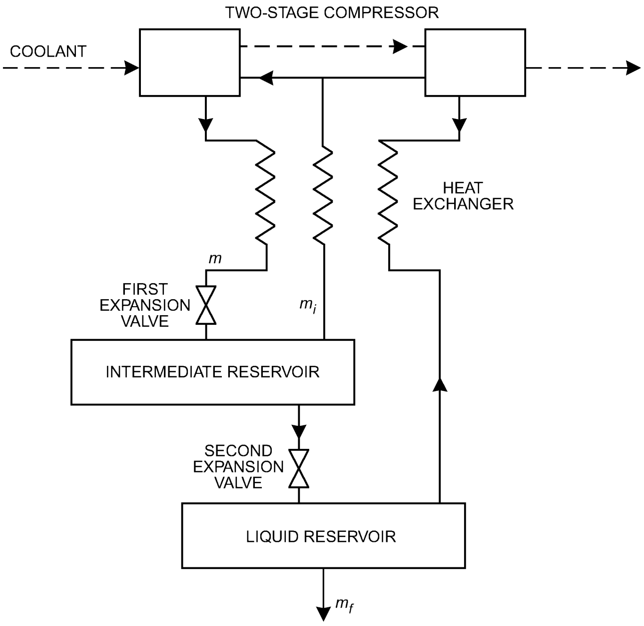

Fig. 14 Dual-Pressure Joule-Thomson Cycle Used as Liquefier

$$\mathrm{COP} = \frac{T_5 - T_4}{T_1 \ln(T_5/T_4) - (T_5 - T_4)} \qquad (12)$$

where the absolute temperatures refer to the designated points shown in Figure 15 and T_1 is the ambient temperature.

Combined Isenthalpic and Isentropic Expansion

To take advantage of the increased reversibility gained by using a work-producing expansion engine while minimizing the problems associated with the formation of liquid in such a device, Claude developed a process that combined both expansion processes in the same cycle. Figure 16 shows a schematic of this cycle and the corresponding temperature-entropy diagram.

An energy balance for this system, which incorporates the heat exchangers, expansion engine, J-T expansion valve, and liquid reservoir, allows evaluation of the refrigeration effect or, in the case of a liquefier, of the liquid yield. For the refrigerator, the refrigeration effect is

$$Q = m(h_1 - h_2) + m_e(h_3 - h_e) \qquad (13)$$

where m_e and h_e are the mass flow rate through the expander and the specific enthalpy of the stream leaving the expander, respectively.

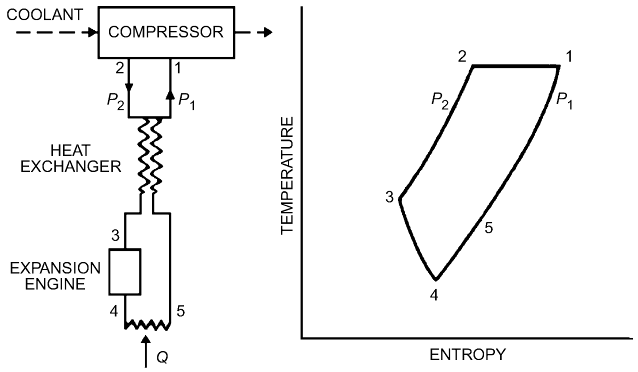

A. SCHEMATIC B. DIAGRAM

Fig. 15 Schematic for Cold-Gas Expansion Refrigerator and Temperature-Entropy Diagram for Cycle

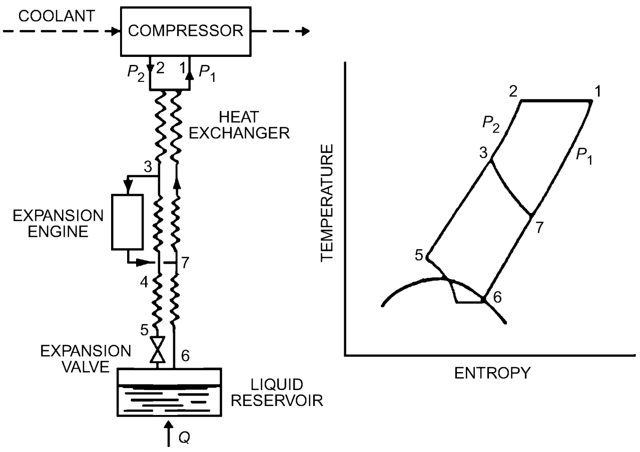

A. SCHEMATIC B. DIAGRAM

Fig. 16 Schematic for Claude Cycle Refrigerator and Temperature-Entropy Diagram for Cycle

For a liquefier, the energy balance yields

$$mh_2 - (m - m_f)h_1 - m_e(h_3 - h_e) - m_f h_f = 0 \qquad (14)$$

Collecting terms and using previously adopted symbols gives the liquid fraction obtained as

$$y = \frac{h_1 - h_2}{h_1 - h_f} - \frac{m_e}{m}\left(\frac{h_3 - h_e}{h_1 - h_f}\right) \qquad (15)$$

For a nonideal expander, the h_e term would be replaced with $h_{e'}$.

One modification of the **Claude cycle** that has been used extensively in high-pressure liquefaction plants for air is the **Heylandt cycle**. In this cycle the first warm heat exchanger in Figure 16 is eliminated, allowing the inlet of the expander to operate at ambient temperatures, which minimizes many of the lubrication problems that are often encountered at lower temperatures.

Other modifications of the basic Claude cycle are replacing the throttling valve with a “wet” expander operating in the two-phase region and adding a saturated vapor compressor after the liquid reservoir. The two-phase expander is used with systems involving helium as the working fluid, because the thermal capacity of the compressed gas is, in many cases, larger than the latent heat of the liquid phase. Experience has shown that operation of the expander with helium in the two-phase region has little effect on expander efficiency as experienced with expanders handling either nitrogen or air. Adding the saturated vapor compressor actually improves the thermodynamic performance of the system.

Another modification of the basic Claude cycle is the **dual-pressure Claude cycle**, similar in principle to the dual-pressure system shown in Figure 14. Only the gas that flows through the expansion valve is compressed to the high pressure; this modification reduces the work requirement per unit mass of gas liquefied. Barron (1985) compared the Claude dual-pressure cycle with the Linde dual-pressure cycle and showed that, in liquefaction of air, the liquid yield can be doubled and the work per unit mass liquefied can be halved when the Claude dual-pressure cycle is selected over the Linde dual-pressure cycle.

Still another extension of the Claude cycle is the **Collins helium liquefier**. Depending on the helium inlet pressure, two to five expansion engines are used in this system. The addition of a liquid nitrogen precooling bath results in a two- to threefold increase in liquefaction performance.

Mixed-Refrigerant Cycle

With the advent of large natural gas liquefaction plants, the mixed-refrigerant cycle (MRC) is the refrigeration process primarily used in LNG production. This cycle, in principle, resembles the cascade cycle occasionally used in LNG production, as shown in Figure 17. After purification, the natural gas stream is cooled by the successive vaporization of propane, ethylene, and methane. These gases have each been liquefied in a conventional refrigeration loop. Each refrigerant may be vaporized at two or three different pressure levels to increase the natural gas cooling efficiency, but at a cost of considerably increased process complexity.

Cooling curves for natural gas liquefaction by the cascade process are shown in Figures 18A and 18B. The cascade cycle efficiency can be improved considerably by increasing the number of refrigerants used. For the same flow rate, the actual work required for the nine-level cascade cycle is approximately 80% of that required by the three-level cascade cycle. This increase in efficiency is achieved by minimizing the temperature difference throughout the cooling curve.

The cascade system can be designed to approximate any cooling curve; that is, the quantity of refrigeration provided at the various temperature levels can be chosen so that the temperature differences between the warm and cold streams in the evaporators and heat exchangers approach a practical minimum (smaller temperature differences equate to lower irreversibilities and therefore lower power consumption).

The simplified version of the mixed-refrigerant cycle shown in Figure 19 is a variation of the cascade cycle. This version involves the circulation of a single mixed-refrigerant system, which is repeatedly condensed, vaporized, separated, and expanded. As a result, these processes require more sophisticated design approaches and more complete knowledge of the thermodynamic properties of gaseous mixtures than expander or cascade cycles. Nevertheless, simplifying compression and heat exchange in such cycles offers potential for reduced capital expenditure over conventional cascade cycles. Note the similarity of the temperature versus enthalpy diagram shown in Figure 20 for the mixed-refrigerant cycle with the corresponding diagram for the nine-level cascade cycle in Figure 18B.

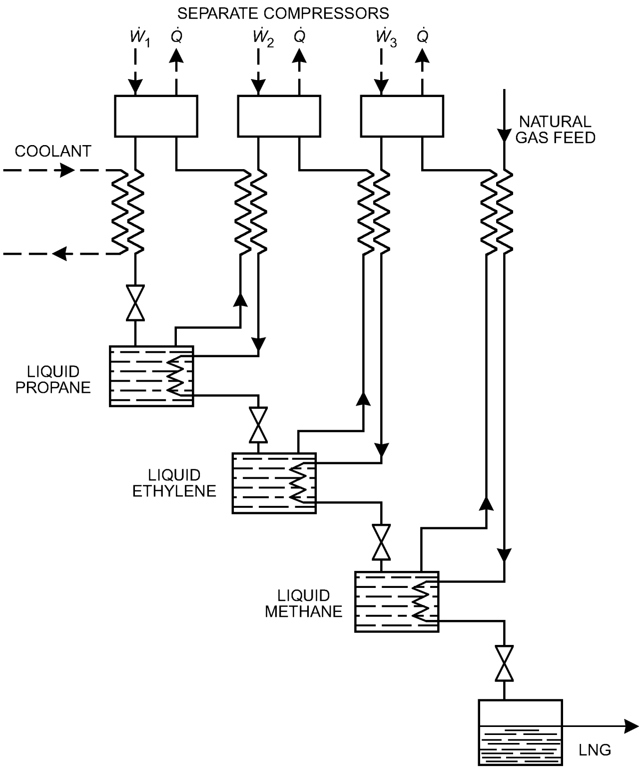

Fig. 17 Classical Cascade Compressed-Vapor Refrigerator

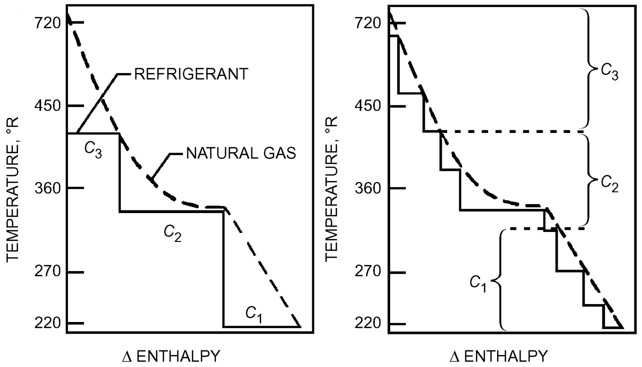

A. THREE-LEVEL CASCADE CYCLE

B. NINE-LEVEL CASCADE CYCLE

Fig. 18 Three-Level and Nine-Level Cascade Cycle Cooling Curves for Natural Gas

Proprietary variations of the mixed refrigerant have been developed. In one commercial process, for example, the gas mixture is obtained by condensing part of the natural gas feed. This has the advantage of requiring no fluid input other than the natural gas itself; however, this procedure can cause a slow start-up because of the refrigerant that must be collected and the time required to adjust its composition. Another version uses a multicomponent refrigerant that is circulated in a completely separate flow loop. The mixture is prepared from pure gaseous components to obtain the desired composition. Thereafter, only occasional makeup gases are added,

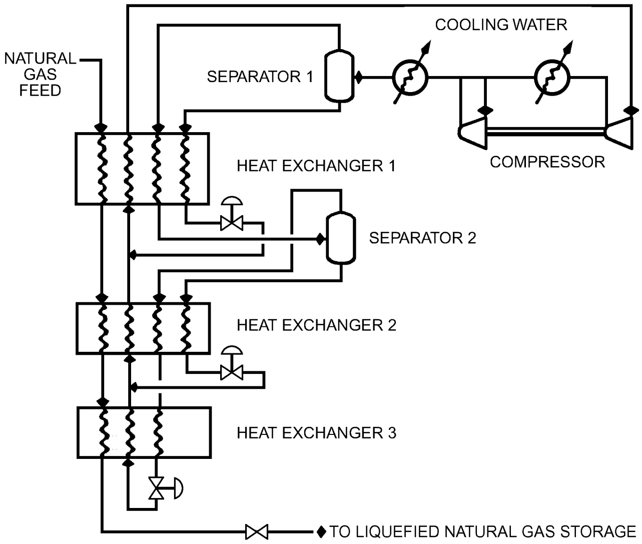

Fig. 19 Mixed-Refrigerant Cycle for Natural Gas Liquefaction

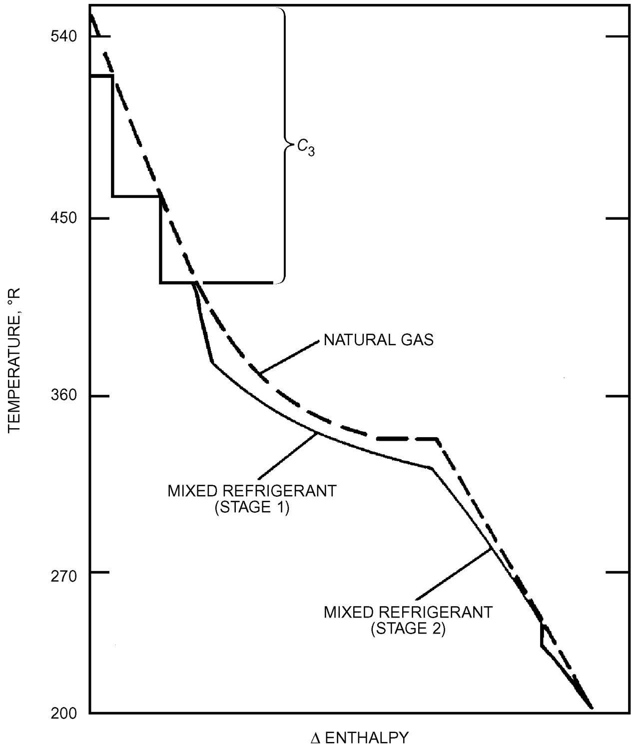

Fig. 20 Propane-Precooled Mixed-Refrigerant Cycle Cooling Curve for Natural Gas Liquefaction

usually from cylinders. This process is simpler and allows for rapid start-up; however, the refrigerant mixture must be stored when the process is shut down. Accordingly, suction and surge drums must be provided, which increases capital expenditure. Gaumer (1986) presents a good review of the mixed-refrigerant cycle.

Comparison of Refrigeration and Liquefaction Systems

The measure of the thermodynamic quality associated with either a piece of equipment or an entire process is its reversibility. The second law, or more precisely the entropy increase, is an effective guide to this degree of irreversibility. However, to obtain a clearer picture of what these entropy increases mean, it is convenient to relate such an analysis to the additional work required to overcome these irreversibilities. The fundamental equation for such an analysis is

$$W = W_{rev} + T_o \sum m\Delta s \qquad (16)$$

where the total work is the sum of the reversible work W_{rev} plus a summation of the losses in availability for various steps in the analysis. Here T_o is the reference temperature (normally ambient), m the flow rate through each individual process step, and Δs the change in specific entropy across these same process steps.

Table 4 Comparison of Several Liquefaction Systems Using Air as Working Fluid

Air Liquefaction System **(Inlet conditions of 70°F and 14.7 psia)**	**Liquid Yield** $y = m_f/m$	**Work per Unit Mass Liquefied, Btu/lb**	**Figure of Merit**
Ideal reversible system	1.000	307	1.000
Simple Linde system p_2 = 2900 psia, η_c = 100%, ε = 1.0	0.086	2253	0.137
Simple Linde system p_2 = 2900 psia, η_c = 70%, ε = 0.95	0.061	4566	0.068
Simple Linde system observed	—	4437	0.070
Precooled simple Linde system p_2 = 2900 psia, T_3 = –49°F, η_c = 100%, ε = 1.00	0.179	963	0.320
Precooled simple Linde system p_2 = 2900 psia, T_3 = –49°F, η_c = 70%, ε = 0.95	0.158	1591	0.194
Precooled simple Linde system, observed	—	2399	0.129
Linde dual-pressure system, p_3 = 2900 psia, p_2 = 870 psia, i = 0.8, η_c = 100%, ε = 1.00	0.060	1180	0.261
Linde dual-pressure system, p_3 = 2900 psia, p_2 = 870 psia, i = 0.8, η_c = 70%, ε = 0.95	0.032	3439	0.090
Linde dual-pressure system, observed	—	2726	0.113
Linde dual-pressure system, precooled to –49°F, observed	—	1539	0.201
Claude system, p_2 = 580 psia, $x = m_e/m$ = 0.7, $\eta_c = \eta_e$ = 100%, ε = 1.00	0.260	383	0.808
Claude system, p_2 = 580 psia, $x = m_e/m$ = 0.7, η_c = 70%, $\eta_{e,ad}$ = 80%, $\eta_{e,m}$ = 90%, ε = 0.95	0.189	868	0.356
Claude system, observed	—	1539	0.201
Cascade system, observed	—	1399	0.221

η_c = compressor overall efficiency
η_e = expander overall efficiency
$\eta_{e,ad}$ = expander adiabatic efficiency
$\eta_{e,m}$ = expander mechanical efficiency
ε = heat exchanger effectiveness
$i = m_i/m$ = mass in intermediate stream divided by mass through compressor
$x = m_e/m$ = mass through expander divided by mass through compressor

Use caution when accepting comparisons made in the literature, because it is difficult to put all processes on a comparable basis. Many assumptions must be made in the course of the calculations, and these can have considerable effect on the conclusions. The most important assumptions generally include heat leak, temperature differences in heat exchangers, efficiencies of compressors and expanders, number of stages of compression, fraction of expander work recovered, and state of flow. For this reason, differences in power requirements of 10 to 20% can readily be due to differences in assumed variables and can negate the advantage of one cycle over another. Table 4 illustrates this point by comparing some of the more common liquefaction systems (described earlier) that use air as the working fluid with a compressor inlet gas temperature and pressure of 70°F and 1 atm (530°R and 14.7 psia), respectively.

To avoid these pitfalls, an analysis should compare the minimum power requirements to produce a unit of refrigeration. Table 5 provides such data for some of the more common cryogens, in addition to the minimum power requirements for liquefaction. The warm temperature in all cases is fixed at 80°F (540°R), and the cold temperature is assumed to be the normal boiling temperature T_{bp} of the fluid. The specific power requirements increase rapidly as the boiling points of the fluids decrease.

Table 5 also shows that more power is required to produce a given amount of cooling with the liquid from a liquefier than is needed for a continuously operating refrigerator. This greater power is needed because less refrigeration effect is available for cooling the feed gas stream when the liquid is evaporated at another location (other than the source of liquefaction itself).

An ideal helium liquefier requires a power input of 3048 Btu/h to produce liquid at the rate of 1 gal/h. Because the heat of vaporization of helium is low, 1 Btu/h will evaporate 0.107 gal/h. Thus, 326 Btu/h would be required to ideally power a liquefier with a liquid product used to absorb 1 Btu/h of refrigeration at –452.4°F (7.6°R). An ideal refrigerator, on the other hand, would only require 70.4 Btu/h of input power to produce the same quantity of refrigeration also at –452.4°F (7.6°R). This difference in power requirement does not mean that a refrigerator will always be chosen over a liquefier for all cooling applications; in some circumstances, a liquefier may be the better or the only choice. For example, a liquefier is required when a constant-temperature bath is used in a low-temperature region. Also, a single centralized liquefier can supply liquid helium to a large number of users.

Another comparison of low-temperature refrigeration examines the ratio of W/Q for a Carnot refrigerator with the ratio obtained for the actual refrigerator. This ratio indicates the extent to which an actual refrigerator approaches ideal performance. (The same ratio can be formed for liquefiers using the values from Table 5 and the actual power consumption per unit flow rate.) This comparison with

Table 5 Reversible Power Requirements

		Ideal Power Input for		
Fluid	T_{bp}, **°R**	**1 Btu/h Refrigerant Capacity,** $\frac{\text{Btu/h}}{\text{Btu/h}}$	**1 gal Liquid,** $\frac{\text{Btu/h}}{\text{gal}}$	**1 Btu/h Refrig. Capacity from Liquid,*** $\frac{\text{Btu/h}}{\text{Btu/h}}$
Helium	7.6	70.4	3048	326
Hydrogen	36.7	13.7	3590	31.7
Neon	48.8	10.1	5773	15.5
Nitrogen	139.3	2.88	2234	3.87
Fluorine	153.0	2.53	3074	3.26
Argon	157.1	2.44	2389	2.95
Oxygen	162.3	2.33	2518	2.89
Methane	201	1.69	1666	2.15

*Obtained by dividing ideal liquefaction power requirement by heat of vaporization of fluid.

ideal performance is plotted in Figure 21 as a function of refrigeration capacity for actual refrigerators and liquefiers. The capacity of the liquefiers included in this comparison was obtained by determining the percent of Carnot performance that these units achieved as liquefiers and then calculating the refrigeration output of a refrigerator operating at the same efficiency with the same power input.

The data for these low-temperature refrigerators cover a wide range of capacity and temperatures. The more efficient facilities are the larger ones that can more advantageously use complex thermodynamic cycles. The same performance potential may exist in the smaller units, but costs are prohibitive and the savings in electrical power have generally not justified the greater capital expenditure.

CRYOCOOLERS

Small, low-temperature refrigerators that provide no more than a few watts of cooling are generally called cryocoolers. Problems of efficiency, unreliability, size, weight, vibration, and cost have been major concerns for cryocooler developers. The seriousness of any one of these problems depends on the application of the cryocooler. The largest application of cryocoolers has been in cooling infrared sensors for night vision in satellites by the military, primarily using Stirling cryocoolers with a refrigeration capacity of about 0.85 Btu/h at −316°F (144°R). These devices have a mean time to failure of about 7500 h (M-CALC IV 2003), but this is inadequate to meet the requirements of space operations and has provided the impetus for major innovations for Stirling units and the rapid growth of research and development of pulse tube refrigerators.

The largest application of cryocoolers in the commercial area has been in cryopumping for the manufacture of semiconductors. Gifford-McMahon cryocoolers (see the section on these cryocoolers under Regenerative Systems) providing a few watts of refrigeration at a temperature of about −433°F (27°R) are the most popular devices for this area. This choice may change, however, because of the vibration characteristics of this cryocooler. Semiconductor manufacturers are forced to achieve narrow line widths in their computer chips to provide more compact packaging of semiconductor circuits.

Even though cryocoolers can be classified by the thermodynamic cycle that is followed, generally there are only two types: recuperative or regenerative units. **Recuperative** cryocoolers use only recuperative heat exchangers; a **regenerative** cryocooler must use at least one regenerative heat exchanger (regenerator) in the unit.

Because recuperative heat exchangers provide two separate flow channels for the refrigerant, refrigerant flow is always continuous and in one direction, analogous to a dc electrical system. This heat exchanger requires either valving with reciprocating compressors and expanders or rotary or turbine compressors and expanders. In regenerative cycles, the refrigerant flow oscillates, analogous to an ac electrical system. This oscillatory effect allows the regenerator matrix to store energy in the matrix for the first half of the cycle and release the energy during the next half. To be effective, the solid matrix material in the regenerator must have high heat capacity and good thermal conductivity. Some advances in both types of cryocoolers are reviewed in the following sections.

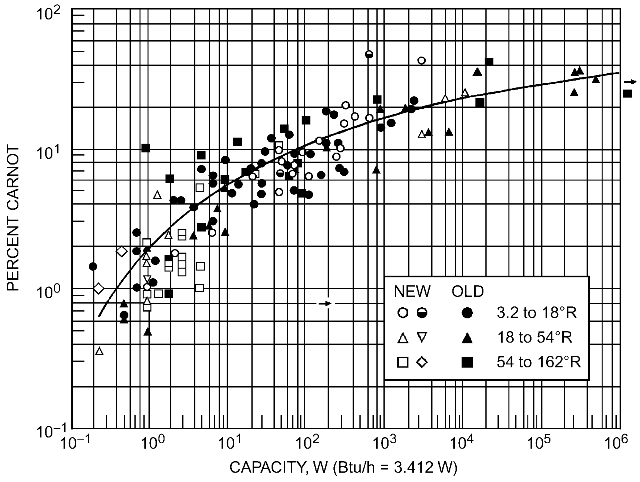

Fig. 21 Efficiency as Percent of Carnot Efficiency
(For low-temperature refrigerators and liquefiers
as function of refrigeration capacity)
(Strobridge 1974)

Recuperative Systems

The J-T and the Brayton cycles, compared schematically in Figure 22, are two recuperative systems.

Joule-Thomson Cryocoolers. The J-T effect of achieving cooling by throttling a nonideal gas is one of the oldest but least efficient methods for attaining cryogenic temperatures. However, J-T cryocoolers have been significantly improved by applying novel methods of fabrication, incorporating more complex cycles, and using special gas mixtures as refrigerants. These developments have made the J-T cryocooler competitive in many applications, even when compared with cryocoolers that generally exhibit more efficient cooling cycles. Their relative simplicity combined with their small size, low mass, and lack of mechanical noise or vibration have been additional advantages for these small refrigerators. In the past, J-T cryocoolers were fabricated by winding a finned capillary tube on a mandrel, attaching an expansion nozzle at the end of the capillary tube, and inserting the entire unit in a tightly fitting tube closed at one end with inlet and exit ports at the other end. Little (1984) introduced a method of fabricating J-T cryocoolers using a photolithographic manufacturing technique in which gas channels for the heat exchangers, expansion capillary, and liquid reservoir are etched on thin, planar glass substrates that are fused together to form a sealed unit. These miniature cryocoolers have been fabricated in a wide range of sizes and capacities. One cryocooler operating at −316°F (144°R) with a refrigeration capacity of 0.8 Btu/h uses a heat exchanger with channels 0.0079 in. wide and 0.0012 in. deep. The channels etched on the glass substrate must be controlled to a tolerance of ±0.00008 in., and the bond between the different substrates must withstand pressures on the order of 2000 to 3000 psia. This cryocooler, used in spot cooling of electronic systems, has an overall dimension of only 3 by 0.55 by 0.08 in (not including the compressor).

Fabrication of miniature J-T cryocoolers by this approach has made it much simpler to use more complex refrigeration cycles and multistage configurations. The dual-pressure J-T cycle, in which the refrigerant pressure is reduced by two isenthalpic expansions, provides either a lower spot-cooling temperature or a higher coefficient of performance for the same power input. Temperatures

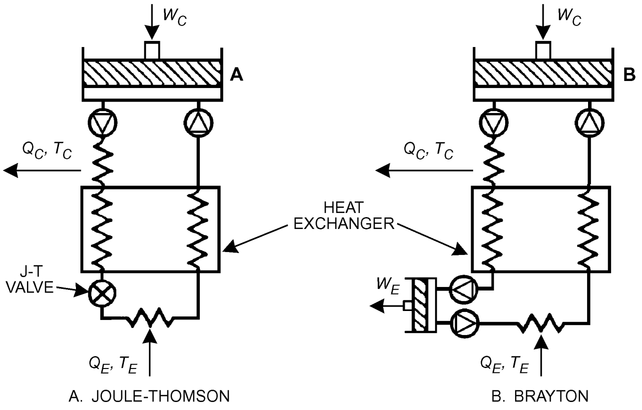

Fig. 22 Schematic of Joule-Thomson and Brayton Cycles
(Two recuperative types of cycles used in cryocoolers)

below –406°F (54°R) have been achieved with two-stage systems. A nitrogen refrigeration stage provides precooling to –321°F (139°R), and a neon J-T stage to achieve operation at –411°F (49°R). Operation at –424°F (36°R) is also possible using hydrogen in place of neon. However, use of multistage units in these miniature cryocoolers requires an order of magnitude better dimensional control of the etching process to match the desired flows and capacities specified for the heat exchangers, expansion capillaries, and liquid reservoirs.

To attain temperatures of –80°F (380°R), pure nitrogen has been used as the refrigerant in J-T cryocoolers. At 80°F (540°R), nitrogen must be compressed to a very high pressure (1500 to 3000 psia) to achieve any significant enthalpy change. The high pressure required leads to a low compression efficiency with high stresses on compressor components, and the small enthalpy change results in a low cycle efficiency. Alfiev et al. (1973), using a gaseous mixture of 30 mol% nitrogen, 30 mol% methane, 20 mol% ethane, and 20 mol% propane, achieved a temperature of –320°F (140°R) using a 50:1 pressure ratio. The system efficiency with this gas mixture was 10 to 12 times better than when pure nitrogen gas was used as the refrigerant. Temperatures below –334°F (126°R) were obtained by adding neon, hydrogen, or helium to the mixture.

Little (1990) established that the addition of the fire retardant CF_3Br (halon) to the nitrogen/hydrocarbon mixture was sufficient to render the mixture nonflammable and was retained in the resulting liquid solution down to –321°F (139°R) or lower without precipitation because of the excellent solvent properties of the mixture. As a result, a series of nitrogen/hydrocarbon gas mixtures that are reasonably safe to use and provide high refrigeration efficiencies were available. However, halon production was discontinued in the United States in 1992 because of its high ozone-depletion potential, and the EPA has additional restrictions on handling recycled halon.

The high cooling capacity of nitrogen/hydrocarbon mixtures is illustrated in the following example. Consider the temperature-entropy diagram shown in Figure 23 for a hydrocarbon mixture of 27% methane, 50% ethane, 13% propane, and 10% butane on a volumetric basis. A throttling process for this gas mixture, initially at 80°F (540°R) and 45 atm (660 psia), can ideally (constant enthalpy) achieve an exit temperature of –100°F (360°R) at a final exit pressure of 1 atm (14.7 psia). Pure nitrogen gas undergoing a similar throttling process from the same inlet conditions to the same final exit pressure only achieves an exit gas temperature of 64°F (524°R). Thus, there can be as much as an elevenfold increase in refrigerant temperature drop after the throttling process by using the gas mixture instead of pure nitrogen gas over these pressure and temperature conditions. That is, refrigeration performance comparable to that using pure nitrogen gas at 1700 to 2000 psia inlet pressures can be achieved with specific gas mixtures at pressure as low as 400 to 700 psia.

The effect of various gas mixture concentrations on the efficiency of any cycle can be analyzed by evaluating the coefficient of performance (COP) of the cycle. The refrigeration effect Q of a J-T refrigerator using such gas mixtures is given by

$$Q = n(h_{lp} - h_{hp})_{min} = n\Delta h_{min} \tag{17}$$

where n is the molar flow rate of the gas mixture, h_{lp} is the molar enthalpy of the low-pressure stream, and h_{hp} is the molar enthalpy of the high-pressure stream at the location in the recuperative heat exchanger that provides a minimum difference in molar enthalpies Δh_{min} between the two streams. The ideal work of compression is evaluated from

$$W_{ideal} = n[(h_2 - h_1) - T_o(s_2 - s_1)] = n\Delta g_o \tag{18}$$

where s_1 and s_2 are the molar entropies at the inlet and outlet from the compressor, respectively, at a constant compression temperature of T_o. The Δg_o is the change in the molar Gibbs free energy also at T_o. The ideal COP of the refrigerant cycle is then

$$\text{COP} = Q/W_{ideal} = \Delta h_{min}/\Delta g_o \tag{19}$$

This indicates that a maximum efficiency in the J-T cycle is achieved when the value of $\Delta h_{min}/\Delta g_o$ is maximized for the refrigerant mixture in the temperature range of interest.

Brayton Cryocoolers. Expanding refrigerant with an expansion engine in the Brayton cycle leads to higher cycle efficiencies than are attainable with J-T cryocoolers. The Brayton cycle is commonly used in large liquefaction systems accompanied by a final J-T expansion. The units are highly reliable because they use turboexpanders operating with gas bearings. For small cryocoolers, the challenge has been in fabricating the miniature turboexpanders while maintaining a high expansion efficiency and minimizing heat leakage. Swift and Sixsmith (1993) addressed this challenge by developing a single-stage Brayton cryocooler with a small turboexpander (rotor diameter of 1/8 in.) providing 17 Btu/h of refrigeration at –343°F (117°R) with neon as the working fluid. The compressor also uses gas bearings with an inlet pressure of 16.2 psia and a pressure ratio of 1.6. The unit operates between –343 and 44°F (117 and 504°R) with a Carnot efficiency of 7.7%. However, the present cost of such cryocoolers limits their service to space applications, which require high reliability, high thermodynamic efficiency, and low vibration.

Mixed-Refrigerant Systems. The possibility of achieving high refrigeration efficiency at cryogenic temperatures with simple closed-cycle J-T (throttle expansion) systems has sparked interest in commercial development of such cryocoolers in the United States. Missimer (1973) described a multistage system in which liquid condensate was withdrawn from the compressed vapor/liquid refrigerant mixture after each of a series of heat exchangers, throttling the withdrawn condensate to a lower pressure, and returning the cold refrigerant to the compressor via counterflow exchangers. Temperatures to 280°R were achieved with this system. However, the system was complicated and has found limited application.

Single-Stage Throttle Expansion Cryocoolers. Longsworth (1997a) described a simple, single-stage throttle expansion refrigerator (see Figure 13) using a single-stage compressor of the type used

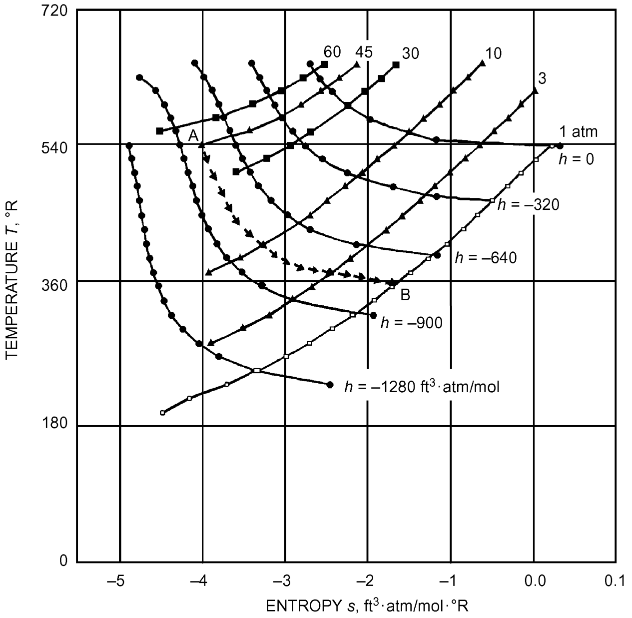

Fig. 23 Isenthalpic Expansion of Multicomponent Gaseous Mixture from A to B

(27% methane, 50% ethane, 13% propane, and 10% butane; *h* is enthalpy) in domestic refrigerators and air-conditioning units. Temperatures to 126°R have been achieved with this system, which evolved out of a Gifford-McMahon (GM) compressor system combined with a J-T heat exchanger. The compressor is oil lubricated, and requires an efficient oil separator and special pretreatment of the oil and system. These additional elements add to the cost of an otherwise simple system (Longsworth 1997b). Over a thousand of these units have been manufactured and are used to cool gamma ray detectors, vacuum system cold traps, infrared (IR) detectors, and laboratory instrumentation.

Alexeev et al. (1999) achieved a refrigeration capacity of 0.03 ton at 180°R with power input of 1100 W using a mixed-refrigerant throttle expansion refrigerator with a precooling stage. This is 18% of Carnot efficiency, and 1.5 times more efficient than a comparable GM refrigerator at the same temperature.

Mixed-Refrigerant Cascade (Kleemenko Cycle) Cryocoolers. Kleemenko (1959) described a one-flow cascade refrigeration cycle using multicomponent refrigerant mixtures. The cycle was based on two key features that promised to give high refrigeration efficiency. As is well known, much of the inefficiency of a throttle expansion system lies in irreversibility of heat transfer in the heat exchanger and in the expansion process. Kleemenko pointed out that heat exchanger inefficiency is exacerbated by the fact that heat capacity of the fluid in the high-pressure stream and of that of the low-pressure stream generally differ, and, as a result, the temperature difference between the two streams diverges along the length of the heat exchanger. If, however, a suitably designed mixture of refrigerants is used instead of a single component, it is possible to keep these two capacities similar and thus minimize the temperature difference between them, reducing the irreversibility. Secondly, he noted that the thermodynamic reversibility of throttling is much greater for a fluid in the liquid state than for one in the gaseous state. He demonstrated the improvement that could be achieved by applying these two factors in a large, liquid natural gas plant.

These factors are the basis for development of a new class of small, low-cost cryocoolers with good efficiency and exceptionally high reliability. The history of this development is given by Little (1998). These coolers use the refrigerant cycle shown in Figure 24. The compressor (1) is an oil-lubricated, hermetically sealed, home refrigerator compressor. Some oil is entrained in the high-pressure refrigerant stream, and most of it is removed in a small cyclone oil separator (2) and returned to the compressor via a small capillary return line (11). The high-pressure vapor is then cooled in the air-cooled condenser (3), where the highest-boiling components of the mixture condense. This two-phase mixture is injected tangentially into the second cyclone separator (4), where the liquid condensate and any remaining oil collect at the bottom, are fed through a short heat exchanger to the throttle expander (6), and ultimately return to the compressor via the line (5) that cools the upper end of the separator. This upper part of the separator is filled with platelets that act as a fractionating column; its large surface area ensures that the vapor and liquid fractions are in equilibrium with one another. Additional refrigerant condenses on these platelets and drips down to the liquid outlet (4), while the remaining vapor exits from the top of the column.

This cleansed vapor then passes to the heat exchanger and is precooled by evaporating liquid from the throttle restrictor (6) in the heat exchanger. It flows through the remainder of the exchanger (7), condensing as it goes, and passes through the second throttle (8) as a liquid, which, upon evaporating, cools the load (9).

An important difference between the Kleemenko cycle cooler and the single-stage throttle expansion cooler is the former's use of the fractionator column to remove residual oil and any other impurities from the vapor stream automatically, and return them to the compressor. In the single-stage cooler, oil is trapped in a zeolite or charcoal absorber, which must be replaced when it is saturated. No such maintenance is needed for the Kleemenko system. This self-cleaning feature (Little 1997a; Little and Sapozhnikov 1998) accounts for the cooler's long life and maintenance-free operation. Continuous operation at 216°R for over 67,000 h has been achieved for early prototypes of these coolers, and over 35,000 h to date for units operating at 144°R (Little 2003). The system's simplicity (having only one liquid/vapor separator, which is at ambient temperature) and the use of common commercial refrigeration components (i.e., compressors, condensers, capillaries, and dewars) has reduced the cost of these cryocoolers to little more than the cost of vapor-compression systems.

Tests at the Naval Research Laboratory of low-cost, long-life cryocoolers developed under a DARPA program found they were exceptionally reliable. Vendors supplied demonstration systems for each of the following cycles: Stirling, Gifford-McMahon, single-stage throttle, Kleemenko cycle, and pulse tube. The only coolers to operate continuously within their specification for the 5000 h test were the Kleemenko coolers (Kawecki and James 1999). These coolers have now logged almost 70,000 h at 216°R and 30,000 h at 144°R to date (Little 2003).

A major advantage of the J-T or throttle expansion cycle coolers over other cryocoolers is the absence of moving parts at the cold end. This is important because cooling is frequently used to reduce noise in sensors or detectors, the performance of which can be degraded by any vibration or noise. For this reason, gamma and x-ray detectors had always been cooled with liquid nitrogen. Now, though, the vibration levels of the Kleemenko cycle cold stage are low enough to be comparable to that of boiling liquid nitrogen (Broerman et al. 2001), enabling their use for these detectors.

Refrigerants in these coolers typically are mixtures of 5 to 10 components. Their thermodynamic properties can be calculated with programs such as SUPERTRAPP and DDMIX (NIST 2002a, 2002b), available from NIST, and other commercial programs. Methods for optimizing their refrigerant properties are also available (Dobak 1998; Keppler et al. 2004; Little 1997). However, in practice, the problem is more complicated. Low-cost compressors are oil-lubricated and contain about 1 lb of oil. Each component of the mixture dissolves to a different extent in the oil, and these solubilities are generally a strong function of temperature. Consequently, the composition of the mixture with which the unit is charged differs from that which circulates during operation, and this composition varies as compressor temperature changes. The problem is exacerbated by the fact that some of the higher-boiling-point components condense in the heat exchanger during cooldown, reducing the fraction of these in the refrigerant that circulates. These factors have to be taken into account in designing the appropriate mixture to charge the units.

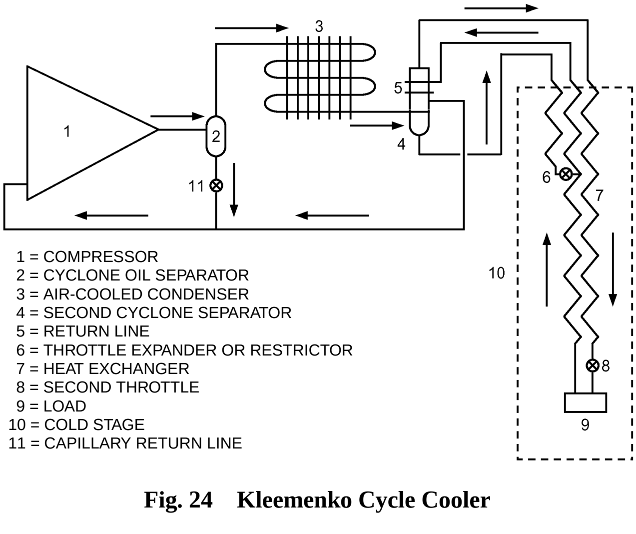

Fig. 24 Kleemenko Cycle Cooler

The low cost, low noise, high reliability, and good efficiency of these new coolers have changed the landscape for cooling in the temperature range from –40 to –330°F. Applications have increased dramatically and now include cryosurgical devices, chip handlers for automated test equipment, low-noise microwave amplifiers, and x-ray and gamma detectors; they have also become the enabling technology for low-cost nitrogen liquefiers for the dermatology market, and oxygen liquefiers for the home care market.

Regenerative Systems

Stirling Cryocoolers. The Stirling refrigerator, which boasts the highest theoretical efficiency of all cryocoolers, is the oldest and most common of the regenerative systems. The elements of the Stirling refrigerator normally include two variable volumes at different temperatures, coupled together through a regenerative heat exchanger, a heat exchanger rejecting the heat of compression, and a refrigerator absorbing the refrigeration effect. These elements can be arranged in a wide variety of configurations and operate as either single- or double-acting systems. The single-acting units are either two-piston or piston-displacer systems, as shown in Figure 25.

The ideal Stirling cycle consists of four processes:

1. Isothermal compression of the refrigerant in the compression space at ambient temperature by rejecting heat Q_c to the surroundings.
2. Constant-volume regenerative cooling, transferring heat from the working fluid to the regenerator matrix. The reduction in temperature at constant volume causes a reduction in pressure.
3. Isothermal expansion in the expansion space at refrigeration temperature T_E. Heat Q_E is absorbed from the surroundings of the expansion space.
4. Constant-volume regenerative heating in which heat is transferred from the regenerator matrix to the working fluid. The increase in temperature at constant volume increases pressure back to the initial conditions.

Successful operation of the cycle requires that volume variations in the expansion space lead those in the compression space.

Thousands of small, single-stage Stirling cryocoolers have been manufactured. Capacities range from about 0.03 to 3.2 Btu/h at –316°F (144°R). The largest units (not including the compressor) are generally no larger than 6 in. in any dimension, and weigh less than 6.5 lb. Power inputs range from 40 to 50 Btu/h per Btu/h of refrigeration, equivalent to an efficiency of 6 to 7% of Carnot limit.

Many recent developments in Stirling cryocoolers have been directed toward improved reliability. In most applications, for example, linear motor drives have replaced rotary drives to reduce moving parts as well as reduce the side forces between the piston and cylinder. Lifetimes of about 4000 h are the norm with linear compressors; however, lifetimes greater than 15,000 h have been achieved by using improved materials for the rubbing contact. Longer lifetimes have been achieved with piston devices by using flexure, gas, or magnetic bearings to center the piston and displacer in the cylinder housing. Davey (1990) reviews the development of these cryocoolers.

Orifice Pulse Tube Refrigerators. Spaceflight applications require lifetimes of 10 to 15 years, low mass, and low energy consumption. These considerations have directed research on the orifice pulse tube refrigerator (OPTR) shown schematically in Figure 26. This unit is a variation of the Stirling cryocooler in which the moving displacer is replaced by a pulse tube, orifice, and reservoir volume. Radebaugh (1990) gives a detailed review of pulse tube refrigerators.

The orifice pulse tube refrigerator operates on a cycle similar to the Stirling cycle, except that proper phasing between mass flow and pressure is established by the passive orifice rather than by the moving displacer. In this cycle, a low-frequency compressor raises the pressure of the helium refrigerant gas to between 70 and 350 psia during the first half of a sinusoidal compression cycle. The oscillating pressure for the OPTR can be provided either by a compressor similar to that used in the Stirling refrigerator, or by a Gifford-McMahon compressor that has been modified with appropriate valving to achieve the required oscillating pressure. The high-pressure gas, after being cooled in the regenerator, adiabatically compresses the gas in the pulse tube.

Approximately one-third of the compressed gas originally in the pulse tube flows through the orifice to the reservoir volume, with the heat of compression being removed in the hot-exchanger. During the latter half of the sinusoidal cycle, the gas in the pulse tube expands adiabatically, which causes a cooling effect. The cold, expanded gas is forced past the cold heat exchanger and a buffer volume of gas that allows a temperature gradient to exist between the hot and cold ends of the pulse tube. Some mixing or turbulence occurs in the buffer volume because the time-averaged enthalpy flow that represents the gross refrigeration capacity is only 55 to 85% of the ideal enthalpy flow.

By assuming simple harmonic pressure, mass flow, and temperature oscillations in the entire pulse tube refrigerator as well as adiabatic operation in the pulse tube itself, researchers at NIST developed an analytical model that reasonably predicts refrigeration performance (Storch and Radebaugh 1988). Thermoacoustic theories include a linear approximation with higher harmonics and realistic heat transfer and viscous effects between the gas and pulse tube wall. Losses accounted for in these models result in a time-averaged enthalpy flow that agrees closely with experimental values.

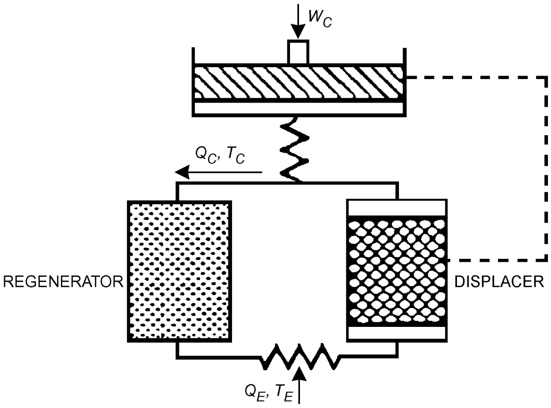

Fig. 25 Schematic of Stirling Cryocooler

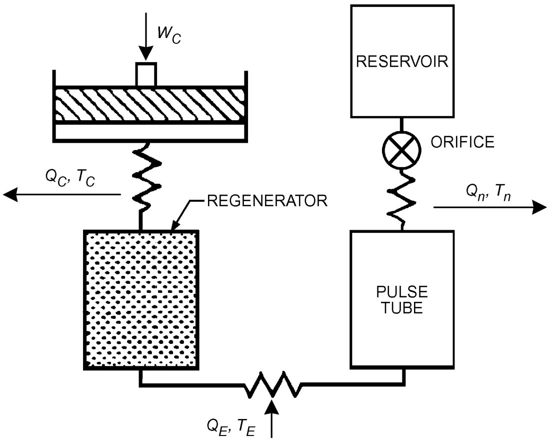

Fig. 26 Schematic for Orifice Pulse Tube Cryocooler

The orifice concept for pulse tube refrigerators achieves a refrigeration temperature of −352°F (108°R) with only one stage. Further refinement can achieve temperatures below −370°F (90°R). However, the improved Stirling refrigerator remains the choice for most spaceflight applications because its Carnot efficiency is typically higher than those obtained from the OPTR.

Zhu et al. (1990) improved efficiencies for pulse tube refrigerators with higher operating frequencies by adding a second orifice, as shown in Figure 27. This double-inlet concept allows gas flow needed to compress and expand the gas at the warm end of the pulse tube to bypass the regenerator and pulse tube. The reduced mass flow through the regenerator reduces regenerator losses, particularly at high frequencies where these losses become large. The second orifice can reduce refrigerator temperature by at least 27 to 36°F in a well-designed pulse tube operating at frequencies of 40 to 60 Hz. This was substantiated in 1994 with a temperature of −425°F (34°R), the lowest temperature achieved to date with a single-stage, double-inlet arrangement.

Figure 28 compares the percent of Carnot efficiency obtained for the improved pulse tube refrigerators with Stirling refrigerators. The shaded area represents the efficiency range obtained for most of the recent Stirling refrigerators, and the circles represent the individual efficiencies obtained from recent pulse tube refrigerators. The highest-power and highest-efficiency unit is the pulse tube refrigerator described by Radebaugh (1995). This unit provided 106 Btu/h of refrigeration at −316°F (144°R) with a rejection temperature of 109°F (569°R), equivalent to a relative Carnot efficiency of 13%. The average operating pressure was 360 psia, and the operating frequency was maintained at 4.5 Hz. The other two circles with lower efficiencies in the −343 to −316°F (117 to 144°R) range represent the efficiencies obtained for the same unit but with different input powers and different cold-end temperatures. The efficiency shown in the −406 to −397°F (54 to 63°R) range is for a small unit developed by Burt and Chan (1995). Even though the data for pulse tube refrigerators are limited, the efficiencies of the most recent pulse tube refrigerators are becoming quite competitive with the best Stirling refrigerators of comparable size.

Two or more pulse tube refrigerator stages are normally used to maintain high efficiency when temperatures below about −370°F (90°R) are desired. Purposes of the staging are to provide net cooling at an intermediate temperature and to intercept regenerator and pulse tube losses at a higher temperature. Three methods exist for the staging arrangement. The first uses a parallel arrangement of a separate regenerator and pulse tube for each stage, with the warm end of each pulse tube at ambient temperature. In the second method, shown in Figure 29, the warm end of the lower-stage pulse tube is thermally anchored to the cold end of the next higher stage in a series configuration. The third method uses a third orifice to permit a fraction of the gas removed from an optimized location in the regenerator to enter the pulse tube at an intermediate temperature. This staging configuration, the multi-inlet arrangement, maintains the simple geometrical arrangement of a single pulse tube, although it would normally require a change in diameter at the tube

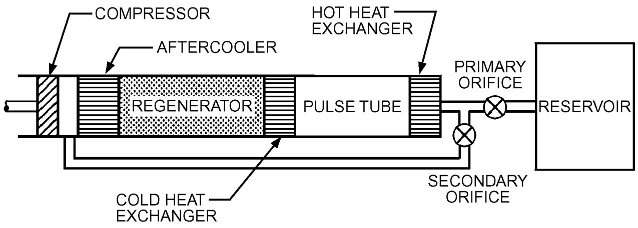

Fig. 27 Schematic of Double-Inlet Pulse Tube Refrigerator Using Secondary Orifice

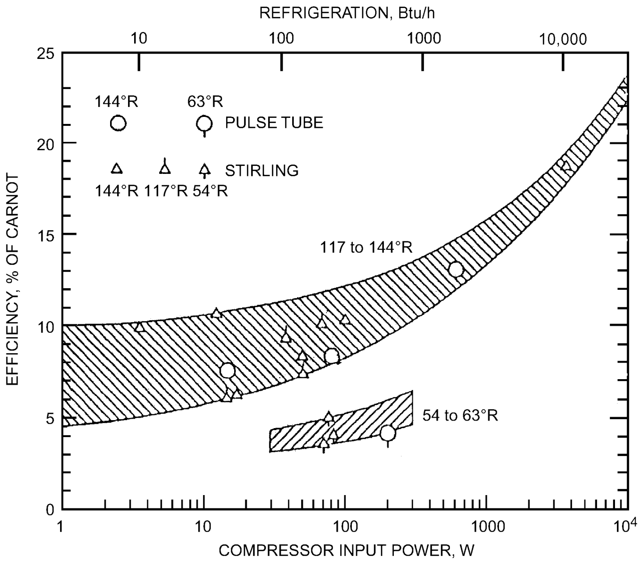

Fig. 28 Comparison of Carnot Efficiency for Several Recent Pulse Tube Cryocoolers with Similarly Powered Stirling Cryocoolers
(Strobridge 1974)

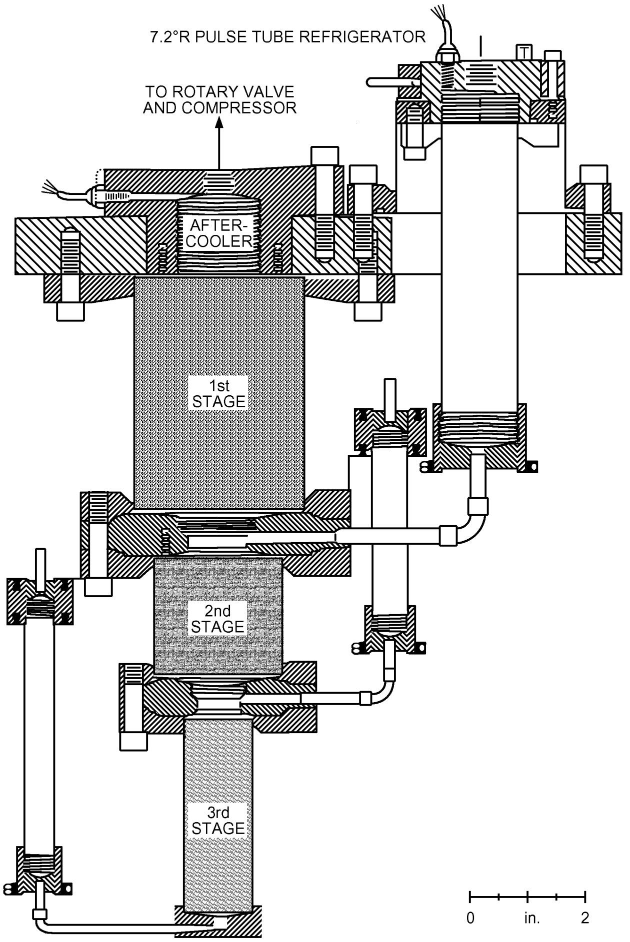

Fig. 29 Three-Stage Series Orifice Pulse Tube Cryocooler for Liquefying Helium

junction with the pulse tube to maintain constant gas velocity in the pulse tube. The lowest temperature attained with a two-stage parallel arrangement of pulse tube refrigerators is –455.7°F (4.0°R).

Gifford-McMahon Refrigerator. J-T cryocoolers using pure gas refrigerants require very high operating pressures; therefore, most commercial closed-cycle cryocoolers use one or more expanders to achieve part of the cooling effect. One of the most widely used regenerative cryocoolers is the Gifford-McMahon refrigerator, schematically shown in Figure 30. These units can achieve temperatures of –343 to –316°F (117 to 144°R) with one stage of expansion and –433 to –453°F (27 to 6.7°R) with two stages of expansion. Precooling the expansion stage is accomplished with regenerators using carefully selected matrix materials. Because regenerators essentially store energy, the matrix materials must possess a high heat capacity as well as a good thermal conductivity. Lead shot has been the regenerator material selected for most regenerative cryocooler operation between –442 to –343°F (18 to 117°R). However, its heat capacity becomes too low to be effective below this temperature range.

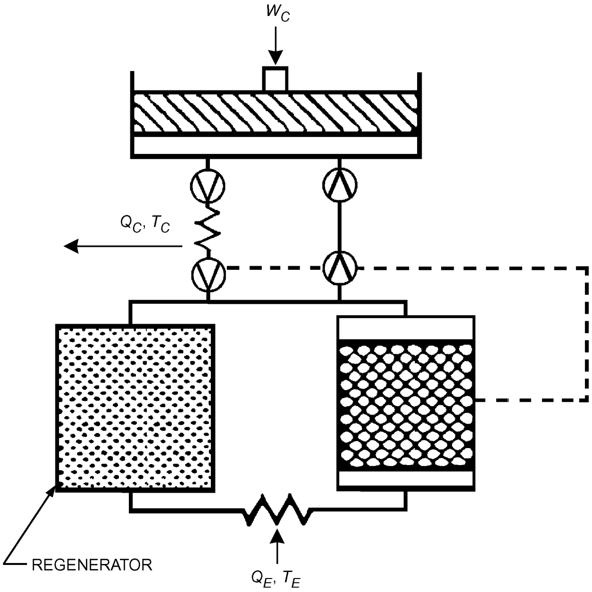

Fig. 30 Schematic for Single-Stage Gifford-McMahon Refrigerator

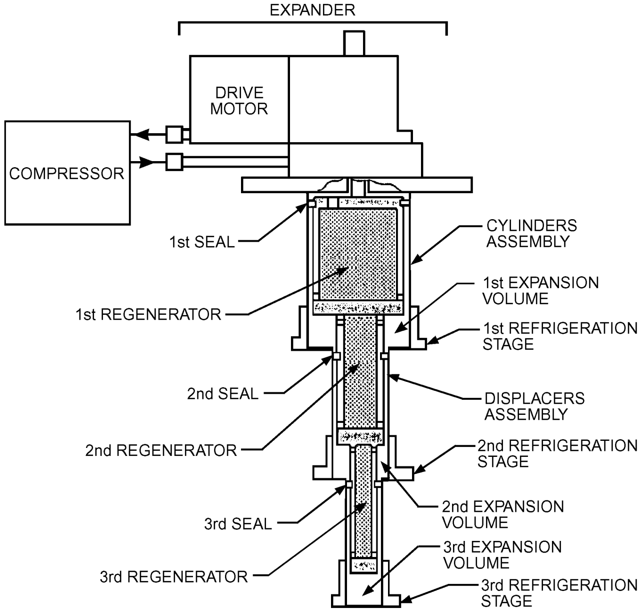

Fig. 31 Cross Section of Three-Stage Gifford-McMahon Refrigerator

Without a suitable matrix material, addition of a third stage with its accompanying regenerator has made it impossible for any regenerative cryocooler to achieve a temperature below –442 to –438°F (18 to 22°R). Attaining a temperature of –452.4°F (7.3°R) to reliquefy helium boil-off has required a two-stage Gifford-McMahon refrigerator equipped with a J-T loop using a compact countercurrent heat exchanger. However, the availability of new matrix materials (rare earth compounds) has made it possible to use a three-stage Gifford-McMahon refrigerator to provide sufficient cooling to reliquefy helium boil-off from superconducting magnets serving MRI units. Nagao et al. (1994) described such a device, shown in Figure 31. It uses $Er_{1.5}Ho_{1.5}Ru$ as the matrix material in the third-stage regenerator and provides a refrigeration capacity of more than 0.5 Btu/h at –452.4°F (7.3°R). This unit, which is smaller than the conventional –453°F (6.7°R) Gifford-McMahon refrigerator, also has greater reliability as well as lower operating costs.

SEPARATION AND PURIFICATION OF GASES

The major application of low-temperature processes in industry involves separation and purification of gases. Much commercial oxygen and nitrogen and all of the neon, argon, krypton, and xenon are separated from air. Pressure-swing adsorption processes account for the oxygen and nitrogen production that is not obtained by cryogenic separation of air. Membranes are also used for small applications in nitrogen production. Commercial helium is separated from helium-bearing natural gas by a low-temperature process. Cryogenics has also been used commercially to separate hydrogen from various sources of impure hydrogen. Even the valuable low-boiling components of natural gas (e.g., methane, ethane, ethylene, propane, propylene) are recovered and purified by various low-temperature schemes. Separation of these gases is dictated by the thermodynamic principles of phase equilibria. The degree to which they separate is based on the physical behavior of the liquid and vapor phases. This behavior is governed, for ideal gas conditions, by the laws of Raoult and Dalton.

The energy required to reversibly separate gas mixtures is the same as the work needed to isothermally compress each component in the mixture from its own partial pressure in the mixture to the final pressure of the mixture. This reversible isothermal work per unit mass is given by the relation

$$(W/m)_i = T_1(s_1 - s_2) - (h_1 - h_2) \qquad (20)$$

where s_1 and h_1 refer to the entropy and enthalpy before separation and s_2 and h_2 refer to the entropy and enthalpy after separation. For a binary system of components A and B, and assuming an ideal gas for both components, Equation (20) simplifies to

$$(W/n_T)_i = -RT\left(n_A \ln\frac{p_T}{p_A} + n_B \ln\frac{p_T}{p_B}\right) \qquad (21)$$

in which n_A and n_B are the moles of components A and B in the mixture, p_A and p_B are the partial pressures of these two components in the mixture, and p_T is the total pressure of the mixture.

The figure of merit for a separation system is defined in a manner similar to that for a liquefaction system, namely

$$\text{FOM} = \frac{(W/m)_i}{(W/m)_{act}} \qquad (22)$$

The number of stages or plates to effect a low-temperature separation is determined by the same procedures as developed for normal separations. A computer is programmed to make interactive mass and energy balances around each plate in a separation column to determine the number of plates required to effect a desired separation. Meaningful computations require accurate thermodynamic data for mixtures and an understanding of the efficiency of separation that can be expected on each plate. Efficiency factors can vary from 65 to 100%.

Air Separation

Figure 32 provides a simplified schematic of the Linde single column originally used for air separation. This cycle produces a high-impurity nitrogen as a by-product. The separation scheme shown uses the simple J-T liquefaction cycle considered earlier but with a rectification column substituted for the liquid reservoir. (Any other liquefaction cycle could have been used in place of the J-T cycle; it is immaterial as to how the liquefied air is furnished to the column). As shown here, purified compressed air is precooled in a three-channel heat exchanger if gaseous oxygen is the desired product. (If liquid oxygen is recovered from the bottom of the column, a two-channel heat exchanger is used for the compressed air and waste nitrogen streams.) The precooled air then flows through a coil in the boiler of the rectifying column, where it is further cooled to saturation while serving as the heat source to vaporize the liquid in the boiler. After leaving the boiler, the compressed fluid expands essentially to atmospheric pressure through a throttling valve and enters the top of the column as reflux for the separation process. Rectification in the column occurs in a manner similar to that observed in ambient-temperature columns. If oxygen gas is to be the product, the air must be compressed to 450 to 900 psia; if it is to be liquid oxygen, pressures of 1500 to 3000 psia are necessary.

Although the oxygen product purity is high from a simple single-column separation scheme, the nitrogen effluent stream always contains about 6 to 7 mol% oxygen. This means that approximately one-third of the oxygen liquefied as feed to the column appears in the nitrogen effluent. This loss is not only undesirable but wasteful in terms of compression requirements. This problem was solved by the introduction of the Linde double-column gas-separation system, in which two columns are placed one on top of the other (Figure 33).

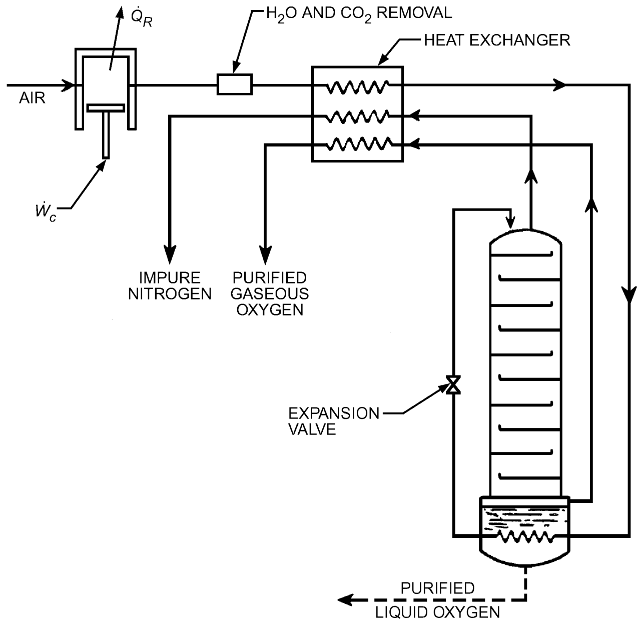

Fig. 32 Linde Single-Column Gas Separator

In this system, liquid air is introduced at an intermediate point in the lower column. A condenser-evaporator at the top of the lower column provides the reflux needed for both columns. Because the condenser must condense nitrogen vapor in the lower column by evaporating liquid oxygen in the upper column, the lower column must operate at a higher pressure (between 75 and 90 psia), while the upper column operates just above 14.7 psia. This requires throttling the overhead nitrogen and the ~45 mol% oxygen products from the lower column as they are transferred to the upper column. The reflux and rectification process in the upper column produce high-purity oxygen at the bottom and high-purity nitrogen at the top of the column, provided that argon and the rare gases have previously been removed.

Figure 34 illustrates the scheme for removing and concentrating the argon. The upper column is tapped at a level where the argon concentration is highest in the column. This gas is fed to an auxiliary column where a large fraction of the argon is separated from the oxygen and nitrogen mixture, which is returned to the appropriate level in the upper column. In modern separation plants, argon is recovered at two purities: either 0.5 or 4% oxygen (by mole). This is called crude argon. Oxygen is readily removed by chemical reduction or adsorption. Nitrogen content is variable, but may be maintained at low levels by proper operation of the upper column. For high-purity argon, the nitrogen must be removed with the aid of another separation column.

Because helium and neon have boiling points considerably below that of nitrogen, these components from the air feed stream collect on the nitrogen side of the condenser-reboiler unit. These gases are recovered by periodically removing a small portion of the gas in the dome of the condenser and sending the gas to a small nitrogen-refrigerated condenser-rectifier. The resulting crude helium and neon are further purified to provide high purity.

Atmospheric air contains only very small concentrations of krypton and xenon. As a consequence, very large amounts of air must be processed to obtain appreciable amounts of these rare gases. Because krypton and xenon tend to collect in the oxygen product, liquid oxygen from the reboiler of the upper column is first sent to an auxiliary condenser-reboiler to increase the concentration of these

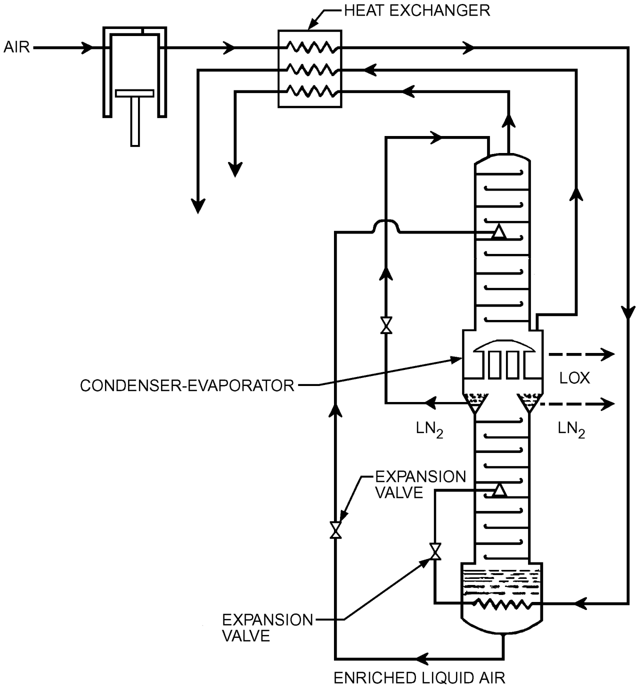

Fig. 33 Traditional Linde Double-Column Gas Separator

two components. The enriched product is further concentrated in another separation column before being vaporized and passed through a catalytic furnace to remove any remaining hydrocarbons with oxygen. The resulting water vapor and carbon dioxide are removed by a caustic trap and the krypton and xenon absorbed in a silica gel trap. The krypton and xenon are finally separated either with another separation column or by a series of adsorptions and desorptions on activated charcoal.

Figure 35 shows a schematic of the double-column gas-separation system presently used to produce gaseous oxygen. Such a column has both theoretical and practical advantages over the Linde double column. A second-law analysis for the two columns shows that the modern double column has fewer irreversibilities than are present in the Linde double column, which results in lower power requirements. From a practical standpoint, only two pressure levels are needed in the modern column, instead of the three required in the Linde double column. A further advantage of the double column in Figure 35 is that it does not require a reboiler in the bottom of the lower column, thereby simplifying the heat transfer process for providing the needed vapor flow in this column. The cooled gaseous air from an expansion turbine provides additional feed to the upper column. High-purity oxygen vapor is available from the vapor space above the liquid in the reboiler of the upper column if impurities in the air stream are removed at the appropriate locations in the column, as with the traditional Linde double-column gas separation system. Further details on modifications made to modern cryogenic air separation plants are given by Grenier and Petit (1986).

Helium Recovery

The major source of helium in the United States is natural gas. Because the major constituents of natural gas have boiling points considerably higher than that of helium, the separation can be accomplished with condenser-evaporators rather than with the more expensive separation columns.

A typical scheme pioneered by the U.S. Bureau of Mines for separating helium from natural gas is shown in Figure 36. In this scheme, the natural gas is treated to remove impurities and compressed to approximately 600 psia. The purified and compressed natural gas stream is then partially condensed by the returning cold low-pressure natural gas stream, throttled to a pressure of 250 psia, and further cooled with cold nitrogen vapor in a heat exchanger separator, where 98% of the gas is liquefied. The cold nitrogen vapor, supplied by an auxiliary refrigeration system, not only provides necessary cooling but also results in some rectification of the gas phase in the heat exchanger, thereby increasing the helium concentration. The remaining vapor phase, consisting of about 60 mol% helium and 40 mol% nitrogen with a very small amount of methane, is warmed to ambient temperature for further purification. The liquid phase, now depleted of helium, furnishes the refrigeration required to cool and partially condense the incoming high-pressure gas. The process is completed by recompressing the stripped natural gas and returning it to the natural gas pipeline with a higher heating value.

The crude helium is purified by compressing the gas to 2700 psia and cooling it first in a heat exchanger and then in a separator that is immersed in a bath of liquid nitrogen. Nearly all of the nitrogen in the crude helium gas mixture is condensed in the separator and removed as a liquid. The latter contains some dissolved helium, which is released and recovered when the pressure is reduced to 250 psia. Helium gas from the separator has a purity of about 98.5 mol%. Final purification to 99.995% is accomplished by sending the cold helium through charcoal adsorption purifiers to remove the nitrogen impurity.

Natural Gas Processing

The need for greater recoveries of the light hydrocarbons in natural gas has led to expanded use of low-temperature processing of these streams. Cryogenic processing of natural gas brings about a phase change and involves physical separation of the newly formed phase from the main stream. The lower the temperature for a given pressure, the greater the selectivity of the phase separation for a particular component.

Most low-temperature natural gas processing uses the turbo-expander cycle to recover light hydrocarbons. Feed gas is normally

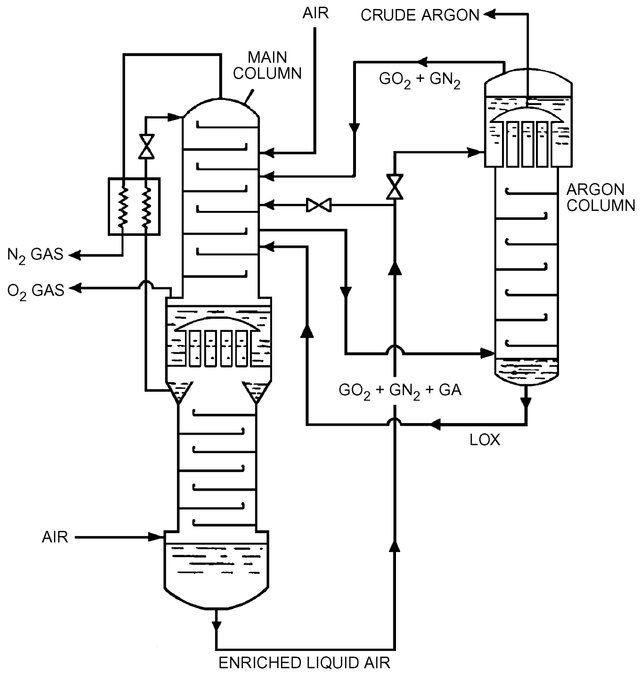

Fig. 34 Argon Recovery Subsystem

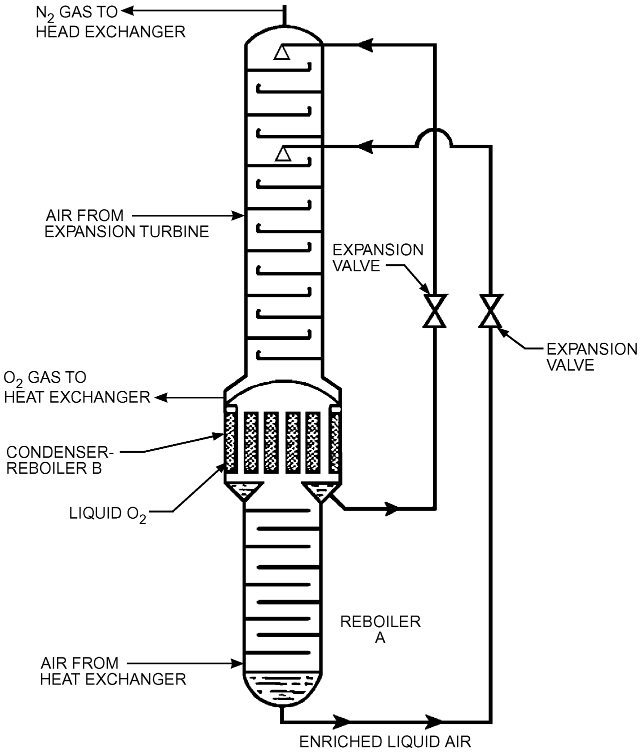

Fig. 35 Contemporary Double-Column Gas Separator

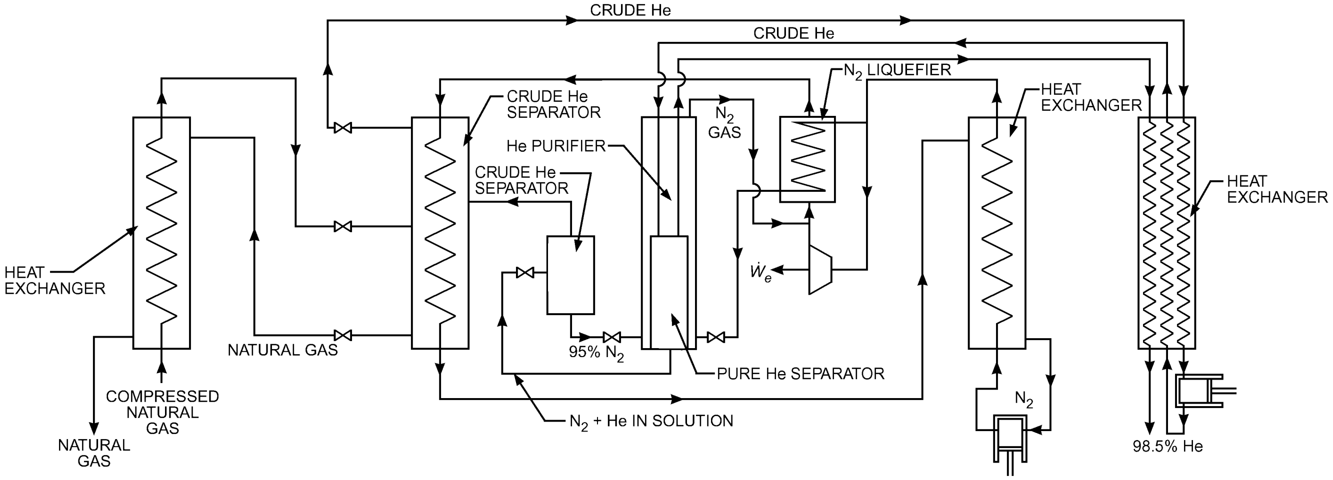

Fig. 36 Schematic of U.S. Bureau of Mines Helium Separation Plant

available from 150 to 1500 psia. The gas is first dehydrated to dew points of –100°F (360°R) and lower. After dehydration, the feed is cooled with cold residue gas. Liquid produced at this point is separated before entering the expander and sent to the condensate stabilizer. Gas from the separator flows to the expander. The expander exhaust stream can contain as much as 20 mass % liquid. This two-phase mixture is sent to the top section of the stabilizer, which separates the two phases. The liquid is used as reflux in this unit, and the cold gas exchanges heat with fresh feed and is recompressed by the expander-driven compressor. Many variations to this cycle are possible and have found practical applications.

Purification Procedures

The nature and concentration of impurities to be removed depend entirely on the process involved. For example, in the production of large amounts of oxygen, impurities such as water and carbon dioxide must be removed to avoid plugging the cold process lines or to avoid build-up of hazardous contaminants. Helium, hydrogen, and neon accumulate on the condensing side of the oxygen reboiler and reduce the rate of heat transfer unless removed by intermittent purging. Acetylene build-up can be dangerous even if the feed concentration of the air is no greater than 0.04 ppm or 4×10^{-8} lb/lb.

Refrigeration purification is a relatively simple method for removing water, carbon dioxide, and other contaminants from a process stream by condensation or freezing. (Either regenerators or reversing heat exchangers may be used for this purpose, because flow reversal is periodically necessary to reevaporate and remove the solid deposits.) Effectiveness depends on the vapor pressure of impurities relative to that of the major process stream components at the refrigeration temperature. Thus, assuming ideal gas behavior, the maximum impurity content in a gas stream after refrigeration would be inversely proportional to its vapor pressure. However, at higher pressures, the impurity content can be significantly greater than that predicted for the ideal situation. Data on this behavior are available as **enhancement factors**, defined as the ratio of the actual molar concentration to the ideal molar concentration of a specific impurity in a given gas.

Purification by a solid adsorbent is one of the most common low-temperature methods for removing impurities. Materials such as silica gel, carbon, and synthetic zeolites (molecular sieves) are widely used as adsorbents because of their extremely large effective surface areas. Carbon and most of the gels have pores of varying sizes in a given sample, but the synthetic zeolites are manufactured with closely controlled pore size openings ranging from 0.4 to about 1.3 nm. This pore size makes them even more selective than other adsorbents because it permits separation of gases on the basis of molecular size.

The equilibrium adsorption capacity of the gels and carbon is a function of temperature, the partial pressure of the gas to be adsorbed, and the properties of the gas. An approximation generally exists between the amount adsorbed per unit of adsorbent and the volatility of the gas being adsorbed. Thus, carbon dioxide would be adsorbed to a greater extent than nitrogen under comparable conditions. In general, the greater the difference in volatility of the gases, the greater the selectivity for the more volatile component.

The design of low-temperature adsorbers requires knowledge of the equilibrium between the solid and the gas and the rate of adsorption. Equilibrium data for the common systems generally are available from the suppliers of such material. The rate of adsorption is usually very rapid and the adsorption is essentially complete in a relatively narrow zone of the adsorber. If the concentration of adsorbed gas is more than a trace, then the heat of adsorption may also be a factor of importance in the design. (The heat of adsorption is usually of the same order as or larger than the normal heat associated with a phase change.) Under such situations, it is generally advisable to design the purification process in two steps: first removing a significant portion of the impurity, either by condensation or chemical reaction, and then completing the purification with a low-temperature adsorption system.

In normal plant operation, at least two adsorption units are used: one is in service while the other is being desorbed of its impurities. In some cases, a third adsorbent unit offers some advantage: one adsorbs, one desorbs, and one is cooled to replace the adsorbing unit as it becomes saturated. Adsorption units are generally cooled by using some of the purified gas, to avoid adsorption of additional impurities during the cooling period.

Low-temperature adsorption systems are used for many applications. For example, such systems are used to remove the last traces of carbon dioxide and hydrocarbons in air separation plants. Adsorbents are also used in hydrogen liquefaction to remove oxygen, nitrogen, methane, and other trace impurities. They are also used in the purification of helium suitable for liquefaction (Grade A) and for ultrapure helium (Grade AAA, 99.999% purity). Adsorption at –397°F (63°R), in fact, yields a helium with less than 2×10^{-9} lb/lb (2 ppb) of neon, which is the only detectable impurity in the helium after this treatment.

Even though most chemical purification methods are not carried out at low temperatures, they are useful in several cryogenic gas separation systems. Ordinarily, water vapor is removed by refrigeration and adsorption methods. However, for small-scale purification, the gas can be passed over a desiccant, which removes water vapor as water of crystallization. In the krypton-xenon purification system, carbon dioxide is removed by passage of the gas through a caustic, such as sodium hydroxide, to form sodium carbonate.

When oxygen is an impurity, it can be removed by reacting with hydrogen in the presence of a catalyst to form water, which is then removed by refrigeration or adsorption. Palladium and metallic nickel have proved to be effective catalysts for the hydrogen/oxygen reaction.

EQUIPMENT

The production and use of low temperatures require the use of highly specialized equipment, including compressors, expanders, heat exchangers, pumps, transfer lines, and storage tanks. As a general rule, design principles applicable at ambient temperature are also valid for low-temperature design. However, underlying each aspect of design must be a thorough understanding of temperature's effects on the properties of the fluids being handled and the materials of construction being selected.

Compression Systems

Compression power accounts for more than 80% of the total energy required to produce industrial gases and liquefy natural gas. The three major types of compressors used today are reciprocating, centrifugal, and screw. No particular type of compressor is generally preferred for all applications. The final selection ultimately depends on the specific application, the effect of plant site, available fuel source and its reliability, existing facilities, and power structure.

The key feature of reciprocating compressors is their adaptability to a wide range of volumes and pressures with high efficiency. Some of the largest units for cryogenic gas production range up to 15,000 bhp. They use the balanced-opposed machine concept in multistage designs with synchronous motor drive. When designed for multistage, multiservice operation, these units incorporate manual or automatic, fixed- or variable-volume clearance packets, and externally actuated unloading devices where required. Balanced-opposed units not only minimize vibrations, resulting in smaller foundations, but also allow compact installation of coolers and piping, further increasing the savings.

Air compressors for constant-speed service normally use piston suction valve loaders for low-pressure lubricated machines. Nonlubricated units require diaphragm-operated unloaders. Medium-pressure compressors for argon and hydrogen often use this type of unloader as well. The trend towards nonlubricating machines has led to piston designs using glass-filled PTFE (polytetrafluoroethylene) rider rings and piston rings, with cooled packing for the piston rods.

Larger units operate as high as 277 rpm with piston speeds for air service up to 850 fpm. Larger compressors with provision for multiple services reduce the number of motors or drivers and minimize the accessory equipment, resulting in lower maintenance cost.

Nonlubricated compressors used in oxygen compression have carbon- or bronze-filled PTFE piston rings and piston rod packing. The suction and discharge valves are specially constructed for oxygen service. The distance pieces that separate the cylinders from the crankcase are purged with an inert gas such as nitrogen, to preclude the possibility of high concentrations of oxygen in the area in the event of excessive rod packing leakage. Compressors for oxygen service are characteristically operated at lower piston speeds of the order of 650 fpm. Maintaining these machines requires rigid control of cleaning procedures and inspection of parts to ensure the absence of oil in the working cylinder and valve assemblies.

Variable-speed engine drives can generally operate over a 10 to 100% range in the design speed with little loss in operating efficiency because compressor fluid friction losses decrease with lower revolutions per minute.

Technological advances achieved in centrifugal compressor design have resulted in improved high-speed compression equipment with capacities exceeding 600,000 cfm in a single unit. Discharge pressure of such units is usually between 60 to 105 psia. Large centrifugal compressors are generally provided with adjustable inlet guide vanes to facilitate capacity reductions of up to 30% while maintaining economical power requirements. Because of their high efficiency, better reliability, and design upgrading, centrifugal compressors have become accepted for low-pressure cryogenic processes such as air separation and base load LNG plants.

Separately driven centrifugal compressors are adaptable to low-pressure cryogenic systems because they can be coupled directly to steam turbine drives, are less critical from the standpoint of foundation design criteria, and lend themselves to gas turbine or combined cycle applications. Isentropic efficiencies of 80 to 85% are usually obtained.

Most screw compressors are oil-lubricated. They either are semihermetic (the motor is located in the same housing as the compressor) or have an open-drive (the motor is located outside of the compressor housing and thus requires a shaft seal). The only moving parts in screw compressors are two intermeshing helical rotors. Because rotary screw compression is a continuous positive-displacement process, no surges are created in the system.

Screw compressors require very little maintenance because the rotors turn at conservative speeds and they are well lubricated with a cooling lubricant. Fortunately, most of the lubricant can easily be separated from the gas in screw compressors. Typically, only small levels of impurities (1 to 2 ppm by weight) remain in the gas after separation. Charcoal filters can be used to reduce the impurities further.

A major advantage of screw compressors is that they can attain high pressure ratios in a single mode. To handle these same large volumes with a reciprocating compressor requires a double-stage unit. Because of this and other advantages, screw compressors are now preferred over reciprocating compressors for helium refrigeration and liquefaction applications. They are competitive with centrifugal compressors in other applications as well.

Expansion Devices

The primary function of a cryogenic expansion device is to reduce gas temperature to provide useful refrigeration for the process. In expansion engines, the temperature is reduced by converting part of the energy of the high-pressure gas stream into mechanical work. In large cryogenic facilities, this work is recovered and used to reduce the overall compression requirements of the process. A gas can also be cooled by expanding it through an expansion valve (provided that its initial temperature is below the inversion temperature of the gas), converting part of the energy of the high-pressure gas stream into kinetic energy. No mechanical work is obtained from such an expansion.

Expanders are of either the reciprocating or the centrifugal type. **Centrifugal expanders** have gradually displaced the reciprocating type in large plants. However, the **reciprocating expander** is still popular for those processes where the inlet temperature is very low, such as for hydrogen or helium gas. Units up to 3600 hp are in service for nitrogen expansion in liquid hydrogen plants, whereas nonlubricated expanders with exhausts well below −400°F (60°R) are used in liquid hydrogen plants developed for the space program.

For reciprocating expanders, efficiencies of 80% are normally quoted; values of 85% are quoted for high-capacity centrifugal types (generally identified as turboexpanders). Usually, reciprocating expanders are selected when the inlet pressure and pressure ratio are high and the volume of gas handled is low. The inlet pressure to expansion engines used in air separation plants varies from 600 to 3000 psia, and capacities range from 200 to 6500 cfm.

The design features of reciprocating expanders used in low-temperature processes include rigid, guided cam-actuated valve gears; renewable hardened valve seats; helical steel or air springs;

and special valve packing that eliminates leakage. Cylinders are normally steel forgings effectively insulated from the rest of the structure. Removable nonmetallic cylinder liners and floating piston design offer wear resistance and good alignment in operation. Piston rider rings serve as guides for the piston. Nonmetallic rings are used for nonlubricated service. Both horizontal and vertical design, and one- and two-cylinder versions, have been used successfully.

Nonlubricated reciprocating expansion engines are generally used whenever possible oil contamination is unacceptable or where extremely low operating temperatures preclude using cylinder lubricants. This type of expansion engine is found in hydrogen and helium liquefaction plants and in helium refrigerators.

Reciprocating expanders in normal operation should not accept liquid in any form during the expansion cycle. However, the reciprocating device can tolerate some liquid for short periods if none of the constituents freeze in the expander cylinder and cause serious mechanical problems. Inlet pressure and temperature must be changed to eliminate any possibility of entering the liquid phase and especially the triple point range on expansion during normal operation.

Turboexpanders are classified as either axial or radial. Most turboexpanders built today are radial, because of their generally lower cost and reduced stresses for a given tip speed. This design allows them to run at higher speeds with higher efficiencies and lower operating costs. On the other hand, axial flow expanders are more suitable for multistage expanders because these units provide an easier flow path from one stage to the next. Where low flow rates and high enthalpy reductions are required, an axial-flow two-stage expander is generally used, with nozzle valves controlling the flow. For example, ethylene gas leaving the demethanizer is normally saturated, and processing expansion conditions cause a liquid product to exit from the expander. Up to 15 to 20% liquid at the isentropic end point can be handled in axial-flow impulse-turbine expanders, so recovery of ethylene is feasible. Depending on the initial temperature and pressure entering the expander and the final exit pressure, good flow expanders can reduce the enthalpy of an expanded fluid by between 75 to 150 Btu/lb, and this may be multistaged. The change in enthalpy drop can be regulated by turbine speed.

Highly reliable and efficient turboexpanders have made large-capacity air separation plants and base-load LNG facilities a reality. Notable advances in turboexpander design center on improved bearings, lubrication, and wheel and rotor design to allow nearly ideal rotor assembly speeds with good reliability. Pressurized labyrinth sealing systems use dry seal gas under pressure mixed with cold gas from the process to provide seal output temperatures above the frost point. Seal systems for oxygen compressors are more complex than those for air or nitrogen and prevent lubricant carryover to the processed gas. By combining variable-area nozzle grouping or partial admission of multiple nozzle grouping, efficiencies up to 85% have been obtained with radial turboexpanders.

Turboalternators were developed to improve the efficiency of small cryogenic refrigeration systems. This is accomplished by converting the kinetic energy in the expanding fluid to electrical energy, which in turn is transferred outside the system where it can be converted to heat and dissipated to an ambient heat sink.

The **expansion valve** (often called the J-T valve) is an important component in any liquefaction system, although not as critical as the others mentioned in this section. This valve resembles a normal valve that has been modified (e.g., exposing the high-pressure stream to the lower part of the valve seat to reduce sealing problems, lengthening the valve stem and surrounding it with a thin-walled tube to reduce heat transfer) to handle the flow of cryogenic fluids.

Heat Exchangers

One of the more critical components of any low-temperature liquefaction and refrigeration system is the heat exchanger. This point is demonstrated by considering the effect of heat exchanger effectiveness on the liquid yield of nitrogen in a simple J-T liquefaction process operating between 15 to 300 psia. The liquid yield under these conditions is zero if the effectiveness of the heat exchanger is less than 85%. (Heat exchanger effectiveness is defined as the ratio of actual heat transfer to the maximum possible heat transfer in the heat exchanger.)

Except for helium II, the behavior of most cryogens may be predicted by using the principles of mechanics and thermodynamics that apply to many fluids at room temperature. This behavior has allowed the formulation of convective heat transfer correlations for low-temperature designs of heat exchangers similar to those used at ambient conditions and ones that use Nusselt, Reynolds, Prandtl, and Grashof numbers.

However, the need to operate more efficiently at low temperatures has made the use of simple exchangers impractical in many cryogenic applications. One of the important advances in cryogenic technology is the development of complex but very efficient heat exchangers. Some of the criteria that have guided the development of these units for low-temperature service are (1) small temperature differences at the cold end of the exchanger to enhance efficiency, (2) large heat exchange surface area to heat exchanger volume ratios to minimize heat leak, (3) high heat transfer rates to reduce surface area, (4) low mass to minimize start-up time, (5) multichannel capability to minimize the number of exchangers, (6) high pressure capability to provide design flexibility, (7) low or reasonable pressure drops in the exchanger to minimize compression requirements, and (8) minimum maintenance to minimize shutdowns.

Minimizing the temperature difference at the cold end of the exchanger has some problems, particularly if the specific heat of the cold fluid increases with increasing temperature, as with hydrogen. In such cases, a temperature pinch, or a minimum temperature difference between the two streams in the heat exchanger, can occur between the warm and cold ends of the heat exchanger. This problem is generally alleviated by adjusting the mass flow of the key stream into the heat exchanger. In other words, the capacity rate is adjusted by controlling the mass flow to offset the change in specific heats. Problems of this nature can be avoided by balancing enthalpy in incremental steps from one end of the exchanger to the other.

Selection of an exchanger for low-temperature operation is normally determined by process design requirements, mechanical design limitations, and economic considerations. The principal industrial exchangers used in cryogenic applications are coiled-tube, plate-fin, reversing, and regenerator units.

Construction. A large number of aluminum tubes are wound around a central core mandrel of a **coiled-tube exchanger**. Each exchanger contains many layers of tubes, along both the principal and radial axes. Pressure drops in the coiled tubes are equalized for each specific stream by using tubes of equal length and carefully varying their spacing in the different layers. A shell over the outer tube layer together with the outside surface of the core mandrel form the annular space in which the tubes are nested. Coiled-tube heat exchangers offer unique advantages, especially for low-temperature conditions where simultaneous heat transfer between more than two streams is desired, a large number of heat transfer units is required, and high operating pressures in various streams are encountered. The geometry of these exchangers can be varied to obtain optimum flow conditions for all streams and still meet heat transfer and pressure drop requirements.

Optimizing a coiled-tube heat exchanger involves variables such as tube and shell flow velocities, tube diameter, tube pitch, and layer spacing. Other considerations include single- and two-phase flow, condensation on either the tube or shell side, and boiling or evaporation on either the tube or shell side. Additional complications occur when multicomponent streams are present, as in natural gas liquefaction, because mass transfer accompanies the heat transfer in the two-phase region.

The largest coiled-tube exchangers contained in one shell have been constructed for LNG base-load service. These exchangers handle liquefaction rates in excess of 60,000 cfm with a heat transfer surface of 250,000 ft^2, an overall length of 200 ft, a maximum diameter of 15 ft, and a mass of over 400,000 lb.

Plate-and-fin heat exchangers are fabricated by stacking layers of corrugated, high-uniformity, die-formed aluminum sheets (fins) between flat aluminum separator plates to form individual flow passages. Each layer is closed at the edge with aluminum bars of appropriate shape and size. Figure 37 illustrates the elements of one layer and the relative position of the components before being joined by brazing to form an integral structure with a series of fluid flow passages. These flow passages are combined at the inlet and exit of the exchanger with common headers. Several sections can be connected to form one large exchanger. The main advantage is that it is compact (about nine times as much surface area per unit volume as conventional shell-and-tube exchangers), yet permits wide design flexibility, involves minimum weight, and allows design pressures to 1000 psia from –453 to 152°F (7 to 612°R).

Fins for these heat exchangers are typically 0.4 in. high and can be manufactured in a variety of configurations that can significantly alter the exchanger's heat transfer and pressure drop characteristics. Various flow patterns can be developed to provide multipass or multistream arrangements by incorporating suitable internal seals, distributors, and external headers. The type of headers used depends on the operating pressures, the number of separate streams involved, and, in the case of counterflow exchangers, whether reversing duty is required.

Plate-and-fin exchangers can be supplied as single units or as manifolded assemblies that consist of multiple units connected in parallel or in series. Sizes of single units are presently limited by manufacturing capabilities and assembly tolerances. Nevertheless, the compact design of brazed aluminum plate-and-fin exchangers makes it possible to furnish more than 350,000 ft^2 of heat transfer surface in one manifolded assembly. These exchangers are used in helium liquefaction, helium extraction from natural gas, hydrogen purification and liquefaction, air separation, and low-temperature hydrocarbon processing. Design details for plate fin exchangers are available in most heat exchanger texts.

Removal of Impurities. Continuous operation of low-temperature processes requires that impurities in feed streams be removed almost completely before cooling the streams to very low temperatures. Removing impurities is necessary because their accumulation in certain parts of the system creates operational difficulties or constitutes potential hazards. Under certain conditions, the necessary purification steps can be accomplished by using reversing heat exchangers.

A typical arrangement of a reversing heat exchanger for an air separation plant is shown in Figure 38. Channels A and B constitute the two main reversing streams. During operation, one of these streams is cyclically changed from one channel to the other. The reversal normally is accomplished by pneumatically operated valves on the warm end and by check valves on the cold end of the exchanger. The warm-end valves are actuated by a timing device, which is set to a period such that the pressure drop in the feed channel is prevented from increasing beyond a certain value because of the accumulation of impurities. Feed enters the warm end of the exchanger and as it is progressively cooled, impurities are deposited on the cold surface of the exchanger. When the flows are reversed, the return stream reevaporates deposited impurities and removes them from the system.

Proper functioning of the reversing exchanger depends on the relationship between the pressures and temperatures of the two streams. Because pressures are normally fixed by other considerations, the purification function of the exchanger is usually controlled by proper selection of temperature differences throughout the exchanger. These differences must be such that, at every point in the exchanger where reevaporation takes place, the vapor pressure of the impurity must be greater than the partial pressure of the impurity in the scavenging stream. Thus, a set of critical values for the temperature differences exists, depending on the pressures and temperatures of the two streams. Because ideal equilibrium concentrations can never be attained in an exchanger of finite length, allowances must be made for an exit concentration in the scavenging stream sufficiently below the equilibrium one. Generally, a value close to 85% of equilibrium is selected.

The use of regenerators was proposed by Frankl in the 1920s for simultaneous cooling and purification of gases in low-temperature processes. In contrast to reversing heat exchangers, in which the flows of the two fluids are continuous and countercurrent during any period, the regenerator operates periodically by storing heat in a high-heat-capacity packing in one half of the cycle and then releasing this stored heat to the fluid in the other half of the cycle. Such an

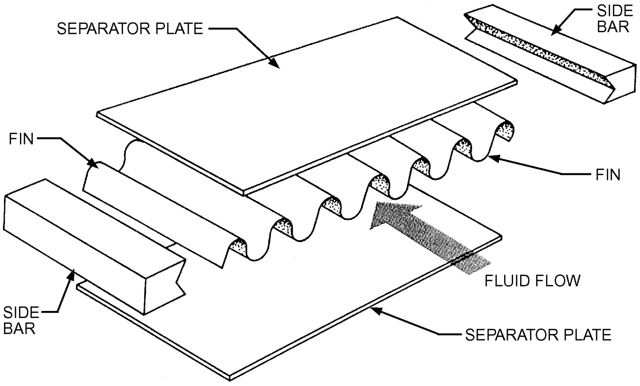

Fig. 37 Enlarged View of One Layer of Plate-and-Fin Heat Exchanger Before Assembly

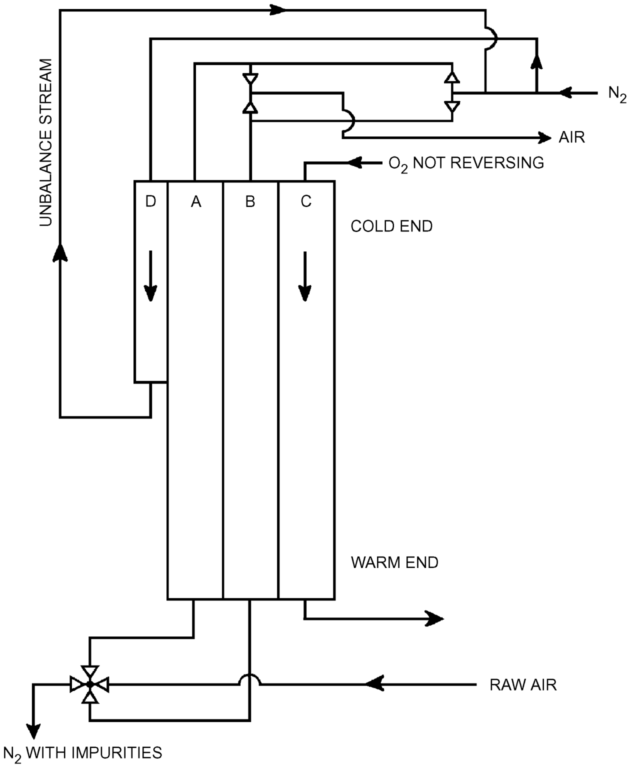

Fig. 38 Typical Flow Arrangement for Reversing Heat Exchanger in Air Separation Plant

exchanger, shown in Figure 39, consists of two identical columns packed with typical matrix materials such as metal screens or lead shot, through which a cyclical flow of gases is maintained. In cooldown, the warm feed stream deposits impurities on the cold surface of the packing. When the streams are switched, the impurities reevaporate as the cold stream is warmed while cooling the packing. Thus, the purifying action of the regenerator is based on the same principles as the reversing exchanger, and the same limiting critical temperature differences must be observed if complete reevaporation of the impurities is to take place.

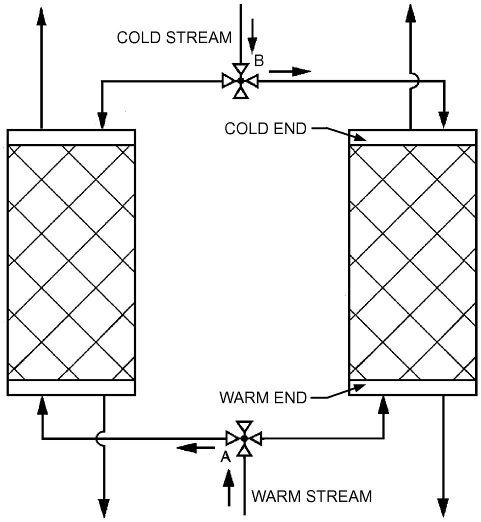

Fig. 39 Flow Arrangement in Regenerator Operation

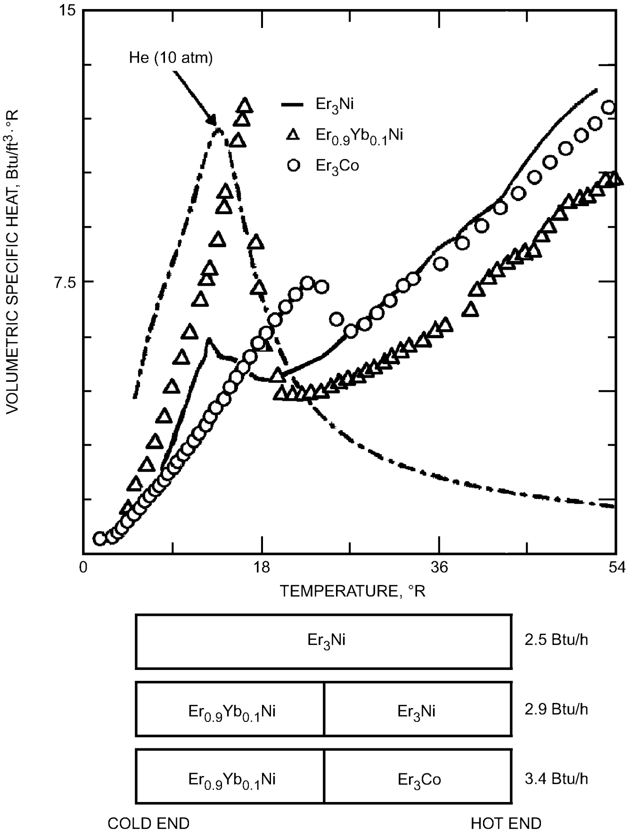

Fig. 40 Specific Heat of Several Rare Earth Matrix Materials
(Kuriyama et al. 1994; reprinted by permission of Springer Science and Business Media))

Regenerators frequently are selected for applications in which the heat transfer effectiveness, defined as Q_{actual}/Q_{ideal}, must be greater than 0.98. A high regenerator effectiveness requires a matrix material with a high heat capacity per unit volume and also a large surface area per unit volume. Until the early 1990s, recuperative heat exchangers rather than regenerators were used in cryocoolers, because the heat capacity of typical matrix materials rapidly decreases to a negligible value below –442°F (18°R). Because an increase in specific heat of a material can only occur when a physical transition occurs in the material, studies have been directed to heavy rare earth compounds that exhibit a magnetic phase transition at these low temperatures. Some of the experimental results are shown in Figure 40. Hashimoto et al. (1992) determined that specific heats of the $ErNi_{i-x}Co_x$ system are more than twice the values obtained for Er_3Ni at –448°F (12°R). Kuriyama et al. (1994) used layered rare earth matrix materials with higher heat capacities than Er_3Ni by itself in the cold end of the second stage of a Gifford-McMahon refrigerator and increased the refrigeration power of the refrigerator by as much as 40% at –453°F (7°R).

The low cost of the heat transfer surface along with the low pressure drop are the principal advantages of regenerators. However, contamination of fluid streams by mixing caused by periodic flow reversals and the difficulty of designing a regenerator to handle three or more fluids has restricted its use and favored the adoption of the plate-and-fin exchangers for air separation plants.

LOW-TEMPERATURE INSULATIONS

The effectiveness of a liquefier or refrigerator depends largely on the amount of heat leaking into the system. Because heat removal becomes more costly as temperature is reduced (the Carnot limitation), most cryogenic systems include some form of insulation to minimize this effect. Cryogenic insulations can be divided into five general categories: high-vacuum, multilayer evacuated insulation, evacuated powder, homogeneous material insulation (cellular glass, polyisocyanurate foam), and composite material systems insulations. The type of insulation chosen for a given cryogenic use depends on the specific application. Homogeneous or composite insulation material itself is only part of a system; other components (e.g., joint sealant, vapor retarder jacketing) need equal consideration to achieve the design goal. Generally, insulation performance is determined by material properties such as thermal conductivity, emissivity, percent moisture content by volume, evacuability, porosity, water vapor permeability, and flammability. In cryogenic service, the dimensional stability and coefficient of linear thermal expansion/contraction of a material are also of particular importance.

Heat flows through an insulation by solid conduction, gas conduction (convection), and radiation. Because these heat transfer mechanisms operate simultaneously and interact with each other, an apparent thermal conductivity *k* is used to characterize the insulation. The value of *k* is measured experimentally during steady-state heat transfer and evaluated from the basic one-dimensional Fourier equation. An insulation system is exposed to cold temperatures on the process side and warm temperatures on the ambient side. Consequently, thermal conductivity at the mean temperature of the application is used in calculating the insulation thickness. The mean temperature is determined by adding the process temperature to the ambient temperature, then dividing by two. Each homogeneous or composite material insulation has an associated polynomial equation to generate its thermal conductivity curve. Basically, thermal conductivity is a data point on a particular material curve at a certain mean temperature. ASTM *Standard* C1045 is the standard for this curve, and calculation methods are based on the ASTM *Standard* C680 methodology. Commercially available software packages can

Table 6 Apparent Thermal Conductivity of Selected Insulations

Type of Insulation	Apparent Thermal Conductivity k_a (between –200 and 75°F mean temperature), Btu/h·ft·°F	Bulk Density ρ, lb/ft^3
Pure gas (at 1 atm, 324°R)		
n-H_2	0.07	0.0082
N_2	0.00042	0.119
Pure vacuum ($p = 10^{-6}$ torr or less)	0.00983	Nil
Foam insulation		
Polystyrene foam	0.0104 to 0.0216	1.6 to 2.2
Polyisocyanurate	0.0117 to 0.0158	1.6 to 8
Cellular glass	0.0242 to 0.0267	7 to 9
Evacuated powder		
Perlite ($p = 10^{-3}$ torr)	0.0006 to 0.0016	4 to 9
Silica ($p = 10^{-3}$ torr)	0.00098 to 0.00121	4 to 6
Multilayer evacuated insulation		
Aluminum foil and fiberglass		
(30–71 layers/in., $p = 10^{-6}$ torr)	0.00002 to 0.00004	4 to 7
(76–152 layers/in., $p = 10^{-6}$ torr)	0.00001	7.5
Aluminum foil and nylon net		
(81 layers/in., $p = 10^{-6}$ torr)	0.00002	5.6

do the calculations on this basis. Insulation manufacturers characterize materials at a thermal conductivity reported at a 75°F mean temperature. This value can be used for comparative purposes between materials at that temperature, but should not be used in cryogenic design. Material manufacturers should be able to provide thermal and property data for performance at cryogenic temperatures. Typical k values for a variety of insulations used in cryogenic service are presented in Table 6.

High-Vacuum Insulation

The mechanism of heat transfer prevailing across an evacuated space (10^{-5} torr or less) is by radiation and conduction through the residual gas. Radiation is generally the more predominant mechanism and can be approximated by

$$\frac{q_r}{A_1} = \sigma\left(T_2^4 - T_1^4\right)\left[\frac{1}{\varepsilon_1} + \frac{A_1}{A_2}\left(\frac{1}{\varepsilon_2} - 1\right)\right]^{-1} \qquad (23)$$

where q_r/A_1 is the radiant heat flux, σ the Stefan-Boltzmann constant, and ε the emissivity of the surface. The subscripts 1 and 2 refer to the cold and warm surfaces, respectively. The bracketed term on the right is the emissivity for an evacuated space with diffuse radiation between spheres or cylinders (with length much greater than diameter). At pressures below 10^{-5} torr, the heat transferred by a gas is directly proportional to the gas pressure and temperature difference. When the molecular mean-free path is much larger than characteristic dimension of the body, molecules that impinge on the body and are then reemitted will, on average, travel a long distance before colliding with other molecules.

The number of reemitted molecules depends on the interaction between the impinging particles and the surface. Gaseous heat conduction under free molecular conditions for most cryogenic applications is given by

$$\frac{q_{gc}}{A_1} = \frac{\gamma + 1}{\gamma - 1}\left(\frac{R}{8\pi MT}\right)^{1/2} \alpha p(T_2 - T_1) \qquad (24)$$

where α, the overall accommodation coefficient, is defined by

$$\alpha = \frac{\alpha_1 \alpha_2}{\alpha_2 + \alpha_1(1 - \alpha_2)(A_1/A_2)} \qquad (25)$$

Table 7 Accommodation Coefficients for Several Gases

Temperature, °R	Helium	Hydrogen	Air
540	0.29	0.29	0.8 to 0.9
140	0.42	0.53	1
36	0.59	0.97	1

and γ is the ratio of the heat capacities, R the molar gas constant, M the relative molecular mass of the gas, and T the temperature of the gas at the point where the pressure p is measured. A_1 and A_2, T_1 and T_2, and α_1 and α_2 are the areas, temperatures, and accommodation coefficients of the cold and warm surfaces, respectively. The accommodation coefficient depends on the specific gas surface combination and the surface temperature. It is defined as representing the fractional extent to which those molecules that fall on the surface and are reflected or reemitted from it have their mean energy adjusted or "accommodated" toward what it would be if the returning molecules were issuing as a stream out of a mass of gas at the temperature of the wall. Table 7 presents accommodation coefficients of three gases at several temperatures.

Heat transfer across an evacuated space by radiation can be reduced significantly by inserting one or more low-emissivity floating shields within the evacuated space. These shields reduce the emissivity factor. The only limitations on the number of floating shields used are system complexity and cost.

Evacuated Multilayer Insulations

Multilayer insulation provides the most effective thermal protection available for cryogenic storage and transfer systems. It consists of alternating layers of highly reflective material, such as aluminum foil or aluminized polyester film, and a low-conductivity spacer material or insulator, such as submicron-diameter glass fibers, paper, glass fabric, or nylon net, all under high vacuum. (The desired vacuum of 10^{-6} torr or less is maintained by using a getter such as activated charcoal to adsorb gases that desorb from the surfaces within the evacuated space.) When properly applied at the optimum density, this type of insulation can have an apparent thermal conductivity as low as 0.00001 to 0.00004 Btu/h·ft·°R between –424 and 80°F (36 and 540°R). The very low thermal conductivity of multilayer insulations can be attributed to the fact that all modes of heat transfer are reduced to a minimum.

The apparent thermal conductivity of a highly evacuated (pressures on the order of 10^{-6} in. Hg or less) multilayer insulation can be determined from

$$k_a = \frac{1}{N/\Delta x}\left\{h_s + \frac{\sigma e T_2^3}{2 - \varepsilon}\left[1 + \left(\frac{T_1}{T_2}\right)^2\right]\left(1 + \frac{T_1}{T_2}\right)\right\} \qquad (26)$$

where $N/\Delta x$ is the number of complete layers (reflecting shield plus spacer) of insulation per unit thickness, h_s the solid conductance for the spacer material, σ the Stefan-Boltzmann constant, ε the effective emissivity of the reflecting shield, and T_2 and T_1 the absolute temperatures of the warm and cold surfaces of the insulation, respectively. Equation (26) indicates that apparent thermal conductivity is inversely proportional to the number of complete layers used in the evacuated space. However, as the multilayer insulation is compressed, the increase in solid conductivity outweighs the decrease in radiative heat, thereby establishing an optimum layer density.

The effective thermal conductivity values generally obtained with actual cryogenic storage and transfer systems often are at least a factor of two greater than the thermal conductivity values shown in Figure 41, which were obtained under carefully controlled conditions. This degradation in insulation thermal performance is caused by the combined presence of edge exposure to isothermal boundaries, gaps, joints, or penetrations in the insulation blanket required for structural supports, fill and vent lines, and the high lateral thermal conductivity of these insulation systems.

Evacuated Powder and Fibrous Insulations

The difficulties encountered with applying multilayer insulation to complex structural storage and transfer systems can be minimized by using evacuated powder or fibrous insulation. This substitution in insulation materials, however, decreases the overall thermal effectiveness of the insulation system by tenfold.

A powder insulation system consists of a finely divided particulate material such as perlite, colloidal silica, calcium silicate, diatomaceous earth, or carbon black inserted between the surfaces to be insulated. When used at 14.7 psia gas pressure (generally with an inert gas), the powder reduces both convection and radiation and, if the particle size is sufficiently small, can also reduce the mean free path of the gas molecules. The apparent thermal conductivity of gas-filled powders is given by the expression

$$k_a = \left[\frac{V_r}{k_s} + \frac{1}{k_g/(1 - V_r) + 4\sigma T^3 d/V_r} \right] \tag{27}$$

where V_r is the ratio of the solid powder volume to the total volume, k_s the thermal conductivity of the powder, k_g the thermal conductivity of the residual gas, σ the Stefan-Boltzmann constant, T the mean temperature of the insulation, and d the mean diameter of the individual powder particles.

The insulating value of powders is increased considerably by removing the interstitial gas. Thus, when powders are used at pressures of 10^{-3} torr or less, gas conduction is negligible and heat transport is mainly by radiation and solid conduction. Figure 42 shows the apparent thermal conductivity of several powders as a function of interstitial gas pressure.

The radiation contribution for evacuated powders near room temperature is larger than the solid conduction contribution to the total heat transfer rate. On the other hand, the radiant contribution is smaller than the solid conduction contribution for temperatures between –321 and –424 or –453°F (139 and 36 or 7°R). Thus, evacuated powders can be superior to vacuum alone (for insulation thicknesses greater than 4 in.) for heat transfer between ambient and liquid nitrogen temperatures. Conversely, because solid conduction becomes predominant at lower temperatures, vacuum alone is usually better for reducing heat transfer between two cryogenic temperatures.

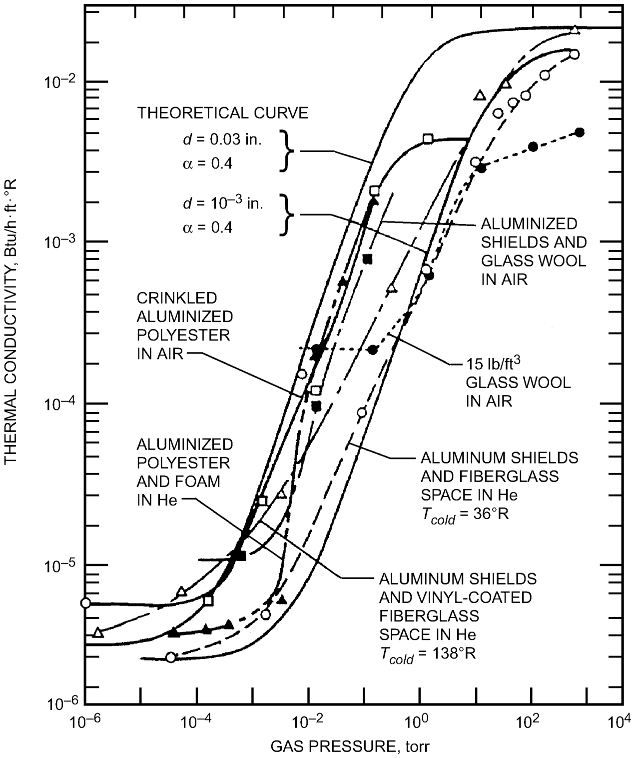

Fig. 41 Effect of Residual Gas Pressure on Apparent Thermal Conductivity of Multilayer Insulation

Very similar considerations govern the use of both powder and fiber insulations. When fibers are used as spacers for multilayer insulation, they are prepared without any binders or lubricants to reduce the possibility of outgassing.

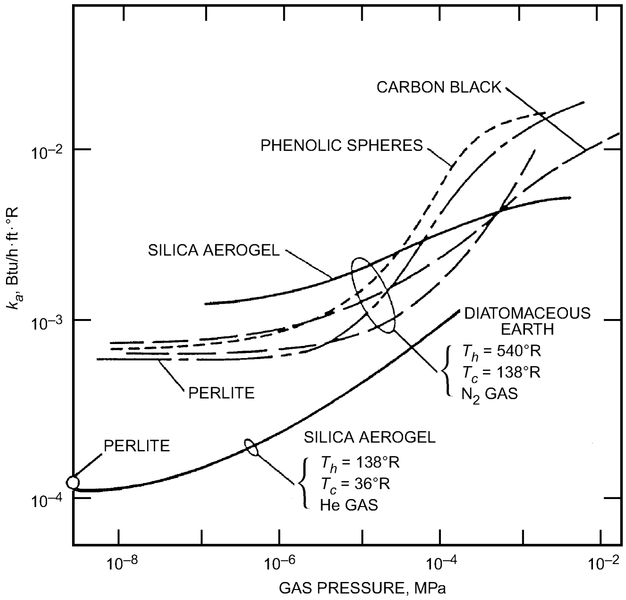

Fig. 42 Apparent Thermal Conductivity of Several Powder Insulations as Function of Residual Gas Pressure

Homogeneous Material Insulations

This category describes materials used in their manufactured state. The most common types of materials used are glass and plastic. Both materials are closed-cell and cellular in structure. Density does not generally affect the performance of homogeneous material insulations in the lower ranges. This does not hold true for high-density inserts used in engineered supports, which typically have densities in the 10 to 20 lb/ft^3 range. These materials have higher thermal conductivities than their lower-density counterparts do. The **coefficient of linear thermal expansion (COLTE)** of the insulation material is one of several important factors to consider when designing the insulation system. The COLTE of each material is a property specific to that material. The design of the insulated system must compensate for differences in expansion/contraction of the insulation versus the pipe metal. Homogeneous material insulations can be used alone or combined with other materials to form a thermal insulation system. The apparent thermal conductivity of homogeneous material insulations depends on the bulk density of the foamed material, the gas contained in the cells (which is a function of age and service temperature of the materials used as the foaming agent), the size of the cells, and the temperature levels to which the insulation is exposed. Heat transport across a foam is determined by convection and radiation in the cells of the foam and by conduction in the solid structure. Evacuation of a foam can effectively reduce its thermal conductivity, provided there is at least a partially open cellular structure, but the resulting values are still considerably higher than either evacuated multilayer, evacuated powder or evacuated fibrous insulations. The opposite effect, diffusion of atmospheric gases into the cells, can increase the apparent thermal conductivity. In particular, the diffusion of hydrogen and helium into the cells can increase the foam's apparent thermal conductivity by a factor of three or four. Of all the foams, polyurethane-modified polyisocyanurates and polystyrene have received the widest use at low temperatures.

When applied to cryogenic systems, some foams tend to crack on repeated thermal cycling and lose their insulation value. The foam material selected must be suitable for the temperature range and cycling conditions expected.

Composite Material Insulations Systems

The optimum insulation system should combine maximum insulation effectiveness, minimum weight, ease of fabrication, and reasonable cost. It would be desirable to use only one insulation material, but because no single insulation has all the desirable physical and strength characteristics required in many applications, composite insulations have been developed. One such insulation consists of a polyurethane foam, reinforcement materials to provide adequate compressive strength, adhesives for sealing and securing the foam to the container, enclosures to prevent damage to the foam from external sources, and vapor barriers to maintain a separation between the foam and atmospheric gases. Another external insulation system for space applications uses honeycomb structures. Phenolic-resin-reinforced fiberglass cloth honeycomb is most commonly used. Filling the cells with a low-density polyurethane foam further improves the thermal effectiveness of the insulation.

STORAGE AND TRANSFER SYSTEMS

Storage vessels range from low-performance containers where the liquid in the container boils away in a few hours to high-performance containers and dewars where less than 0.1% of the fluid contents is evaporated per day.

Storage Systems

The essential elements of a storage vessel consist of an inner vessel, which encloses the cryogenic fluid to be stored, and an outer vessel, which contains the appropriate insulation and serves as a vapor barrier to prevent water and other condensables from reaching the cold inner vessel. The value of the cryogenic liquid stored dictates whether the insulation space is evacuated. In small laboratory dewars designed for liquid nitrogen and oxygen, as shown in Figure 43, insulation is obtained by coating the two surfaces facing the insulation space with low-emissivity materials and then evacuating the space to a pressure of 10^{-6} in. Hg or lower. Laboratory storage of liquid hydrogen and liquid helium, on the other hand, requires evacuated multilayer insulation. In larger vessels, insulations such as powders, evacuated powders, or evacuated multilayer insulations are used, depending on the type of fluid and storage applications. Table 8 provides a tabulation of storage systems based on the preceding criteria.

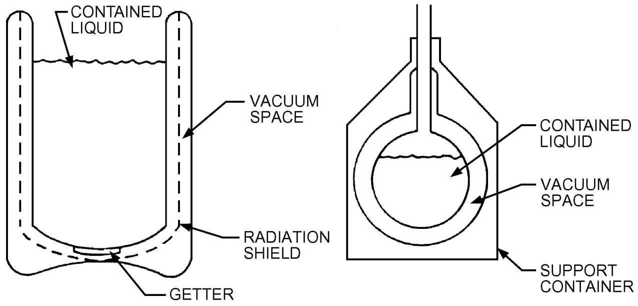

A. OPEN-END DEWAR B. LOX/LIN STORAGE DEWAR

Fig. 43 Laboratory Storage Dewars for Liquid Oxygen and Nitrogen

The transport of cryogens for more than a few hundred feet generally requires specially built transport systems for truck, railroad, or airline delivery. Volumes from 0.7 to more than 3500 ft^3 have been transported successfully by these carriers. Large barges and ships built specifically for shipment of cryogens, particularly LNG, have increased the volume transported manyfold.

Several requirements must be met in the design of the inner vessel. The material of construction must be compatible with the stored cryogen. Nine percent nickel steels are acceptable for high-boiling cryogens ($T > -325$°F); many aluminum alloys and austenitic steels are usually structurally acceptable throughout the entire temperature range. Economic and cooldown considerations dictate that the inner shell be as thin as possible. Accordingly, the inner container is designed to withstand only the internal pressure and bending forces, and stiffening rings are used to support the weight of the fluid. The minimum thickness of the inner shell for a cylindrical vessel under such a design arrangement is given in Section VIII of the ASME (2004) *Boiler and Pressure Vessel Code*.

The outer shell of the storage vessel, on the other hand, is subjected to atmospheric pressure on the outside and evacuated conditions on the inside. Such a pressure difference requires an outer shell of sufficient material thickness with appropriately placed stiffening rings to withstand collapsing or buckling. Again, consult the ASME code for specific design charts.

Heat leaks into cryogen storage vessels by radiation and conduction through the insulation and by conduction through the inner shell supports, piping, instrumentation leads, and access ports. Conduction losses are reduced by making long heat-leak paths, by making the cross-sectional areas for heat flow small, and by using materials with low thermal conductivity. Radiation losses, a major factor in the heat leak through insulations, are reduced by using radiation shields (such as multilayer insulation), boil-off vapor-cooled shields, and opacifiers in powder insulation.

Most storage vessels for cryogens are designed for a 90% liquid volume and a 10% vapor or ullage volume. The latter permits reasonable vaporization of the liquid contents by heat leakage without incurring too rapid a build-up of pressure in the vessel. This, in turn, allows closing the container for short periods either to avoid

Table 8 Insulation Selection for Various Cryogenic Storage Vessels

Fluid	Application	Volume, ft^3	Insulation
Liquid natural gas	Liquefier storage	Up to 57,000	Powder or homogeneous material
	Sea transport	Up to 1.4×10^6	Powder and foam with N_2 purge
Liquid oxygen or nitrogen	Laboratory use	Up to 3.5	Vacuum
	Transport	Up to 7	Multilayer
	Liquefier storage	Up to 1800	Evacuated powder or homogeneous material
	Liquefier storage	Above 1800	Powder or homogeneous material
Liquid hydrogen or helium	Laboratory use	Up to 5.3	Multilayer
Liquid hydrogen	Truck transport	Up to 3500	Multilayer
	Liquefier storage	Up to 134,000	Evacuated powder or homogeneous material
Liquid helium	Truck transport	Up to 1200	Multilayer
	Liquefier storage	Up to 4000	Multilayer

Note: This tabulation should only serve as a guideline; economics will determine the final selection.

partial loss of the contents or to allow the safe transport of flammable or hazardous cryogens.

Transfer Systems

A cryogen is transferred from the storage vessel by one of three methods: self-pressurization of the container, external gas pressurization, or mechanical pumping. Self-pressurization involves removing some of the fluid from the container, vaporizing the extracted fluid, and then reintroducing the vapor into the ullage space to displace the contents of the container. External gas pressurization uses an external gas to displace the container contents. In the mechanical pumping method, the contents of the storage vessel are removed by a cryogenic pump located in the liquid drain line.

Several types of pumps have been used with cryogenic fluids. In general, positive-displacement pumps are best suited for low flow rates at high pressures. Centrifugal or axial-flow pumps are generally best for high-flow applications. Centrifugal or axial-flow pumps have been built and used for liquid hydrogen with flow rates of up to 8000 cfm and pressures of more than 1000 psia. Cryogen subcooling, thermal contraction, lubrication, and compatibility of materials must be considered carefully for successful operation.

Cryogenic fluid transfer lines are generally classified as one of three types: uninsulated, foam-insulated lines, and vacuum-insulated lines. The latter may entail vacuum insulation alone, evacuated powder insulation, or multilayer insulation. A vapor retarder must be applied to the outer surface of foam-insulated transfer lines to minimize insulation degradation that occurs when water vapor and other condensables diffuse through the insulation to the cold surface of the lines.

Cooldown of a transfer line always involves two-phase flow. Severe pressure and flow oscillations occur as the cold liquid comes in contact with the successive warm sections of the line. Such instability continues until the entire transfer line is cooled down and filled with liquid cryogen.

INSTRUMENTATION

Cryogenic instrumentation is used primarily to determine the condition or state of cryogenic fluids, such as pressure and temperature. Such information is typically required for process optimization and control. In addition, the question of quantity and quality transferred or delivered has become commercially important. Accordingly, the instrumentation system must also be able to indicate liquid level, density, and flow rate accurately.

Pressure Measurements

Pressure in cryogenic systems has been measured by simply attaching gage lines from the points where the pressure is to be measured to some convenient location at ambient temperature where a suitable pressure-measuring device is available. This method works well for many applications, but it can have problems of independent frequency response and thermal oscillations. In addition, heat leak, uncertainties in hydrostatic pressure in gage lines, and fatigue failure of gage lines can be significant in some applications. Such problems can be eliminated by installing pressure transducers at the point of measurement. Many pressure transducers used in the cryogenic environment are similar to those used at ambient conditions, such as strain gage and capacitance transducers. However, because pressure-sensing devices often behave quite differently under cryogenic conditions, a systematic testing program can identify the device most suitable for the specific application.

Thermometry

Most low-temperature temperature measurements are made with metallic resistance thermometers, nonmetallic resistance thermometers, or thermocouples. Vapor-pressure thermometers find limited application, but they can provide convenient temperature check points. Important factors in selecting a thermometer include absolute accuracy, reproducibility, sensitivity, heat capacity, self heating, heat conduction, stability, simplicity, response to magnetic field, strain sensitivity, convenience of operation, ruggedness, and cost.

The resistivity of a metallic element or compound varies with a change in temperature. Although many metals are suitable for resistance thermometry, platinum is predominant, mainly because it is chemically inert, easy to fabricate, sensitive down to −424°F (36°R), and very stable.

Many semiconductors, such as germanium, silicon, and carbon, also have useful thermometric properties at low temperatures. Carbon, though not strictly a semiconductor, is included in this group because of its similarity in behavior to semiconductors.

Thermocouples can be very small, so that the disturbance to the object being sensed is very slight and the response time very fast. However, such devices generate rather small voltages, which become smaller as the temperature drops. Copper and constantan is the most commonly used thermocouple pair for low-temperature thermometry, giving an accuracy of ±0.2°F and a sensitivity of 20 μV/°R at room temperature, 9.5 μV/°R at liquid oxygen temperatures, and 3 μV/°R at liquid hydrogen temperatures. Even though other thermocouple combinations such as gold (2.1% atomic cobalt) and copper have larger thermoelectric powers at low temperatures, copper-constantan is still favored because it suffers less from the inhomogeneities common with other thermocouples.

Liquid-Level Measurements

Liquid level is one of several measurements needed to establish the contents of a cryogenic container. Other measurements may include volume as a function of depth, density as a function of physical storage conditions, and, sometimes, useful contents from total contents. Of these measurements, liquid level is presently the most advanced; it can be as accurate and precise as thermometry, and often with greater simplicity.

The operation of cryogenic liquid-level sensors generally depends on a large property change that occurs at the liquid/vapor interface (e.g., a significant change in density). This change may not occur if the fluid is stored near its critical point or if it has stratified after prolonged storage. A convenient way to classify such liquid-level sensors is according to whether the output is discrete (point sensors) or continuous. Point level sensors are tuned to detect sharp property differences and give an on/off signal.

The **capacitance liquid-level sensor** recognizes the differences in dielectric constant between the liquid and the vapor, which is closely related to the fact that the liquid is more dense than the vapor. The **thermal** or **hot wire sensor** detects the large difference in heat transfer between the liquid and vapor phases. The **optical sensor**, on the other hand, detects the change in refractive index between the liquid and the vapor, which is also related to the dielectric constant and density. Several **acoustic** and **ultrasonic devices** operate on the principle that the damping of a vibrating member is greater in liquid than in a vapor.

Continuous liquid-level sensors take many forms. Some sensors determine mass, whereas others are just continuous analogs of some point sensor and merely follow the liquid/vapor interface. Mass sensors include direct weighing, nuclear radiation attenuation, and radio frequency techniques to detect mass. Differential pressure sensors, capacitance, and acoustic devices are used to follow the vapor/liquid interface.

Density Measurements

Measurements of liquid density are closely related to quantity and liquid-level measurements because both are often required simultaneously to establish the mass contents of a tank. The same physical principle may often be used for either measurement, because liquid-level detectors sense the steep density gradient at the liquid/vapor interface. Density may be detected by direct weighing, differential pressure, capacitance, optical or acoustic means, or nuclear radiation attenuation. In general, the various liquid-level principles also apply to density measurement techniques.

Two exceptions are noteworthy. In the case of homogeneous pure fluids, density can usually be determined more accurately by an indirect measurement. That is, density can be calculated from accurate thermophysical properties data by measuring pressure and temperature.

Nonhomogeneous fluids are quite different. LNG, for example, is often a mixture of five or more components with varying composition and, hence, varying density. Accordingly, temperature and pressure measurements alone will not suffice to determine density. In that case, a dynamic, direct measurement, using liquid-level measurement, is required.

Flow Measurements

Three types of flow meters are useful for liquid cryogens: pressure drop or head type, turbine, and momentum.

The **pressure drop** or **head meter** is the oldest method of measuring flowing fluids. Its distinctive feature is a restriction that is used to reduce the static pressure of the flowing fluid. This static pressure difference between the pressures upstream and downstream of the restriction is measured. These meters are simple, and they do not need calibration if proper design, application theory, and practices are followed. Orifice accuracy is generally within ±3% of full scale and repeatability is ±1%. However, transient fluctuation in flow can cause erratic readout, particularly during cooldown and warm-up. Also, static liquid pressures within the meter should be well above the fluid saturation pressure to avoid an erroneous flow measurement from possible cavitation in the flowing stream. In spite of these shortcomings, head meters are widely used and quite reliable.

The **turbine volumetric flow meter** is probably the most popular of the various flow-measuring instruments because of its simple mechanical design and demonstrated repeatability. This meter consists of a freely spinning rotor with multiple blades. The rotor is supported in guides or bearings mounted in a housing that forms a section of the pipeline. The primary requirement is that the angular velocity of the rotor be directly proportional to the volumetric flow rate or, more correctly, to some average velocity of the fluid in the pipe.

Mass-reaction or **momentum-flow meters** are primarily of three types. In one type, an impeller imparts a constant angular momentum to the fluid stream, which is measured as a variable torque on a turbine. In another type, an impeller is driven at a constant torque and the variable angular velocity of the impeller is measured. The third type drives a loop of fluid at either a constant angular speed or a constant oscillatory motion, and the mass reaction is measured. Several of these momentum mass flow meters provide liquid hydrogen mass flow measurement accuracies on the order of ±0.5%. However, two-phase flow degrades mass flow measurement accuracy.

HAZARDS OF CRYOGENIC SYSTEMS

Hazards can best be classified as those associated with the response of the human body and the surroundings to cryogenic fluids and their vapors, and those associated with reactions between certain of the cryogenic fluids and their surroundings.

Physiological Hazards

Exposing the human body to cryogenic fluids or to surfaces cooled by cryogenic fluids can cause severe cold burns (i.e., damage to the skin or tissue similar to that caused by an ordinary burn). Severity of the burn depends on the contact area and contact time: prolonged contact results in deeper burns. Severe burns are seldom sustained if withdrawal is rapid. Cold gases may not be damaging if turbulence in the gas is low, particularly because the body can normally withstand a heat loss of nearly 30 Btu/h·ft^2 for an area of limited exposure. If a burn is inflicted, the only first aid treatment is to liberally flood the affected area with lukewarm water. Massaging the affected area could cause additional damage.

Protective clothing, including safety goggles, gloves, and boots, is imperative for personnel who handle liquid cryogens. Such operations should only be attempted when sufficient personnel are available to monitor the activity.

Whenever the oxygen content of the atmosphere is diluted by nitrogen spills or leaks, there is the danger of nitrogen asphyxiation. Because nitrogen is a colorless, odorless, inert gas, personnel must be aware of associated respiratory and asphyxiation hazards. In general, the oxygen content of air for breathing purposes should be kept between 16 and 25%.

In contrast, an oxygen-enriched atmosphere produces exhilarating effects when breathed. However, lung damage can occur if the oxygen concentration in the air exceeds 60%, and prolonged exposure to an atmosphere of pure oxygen may initiate bronchitis, pneumonia, or lung collapse. Additional threats from oxygen-enriched air are increased flammability and explosion hazards. In this application, the presence of organic materials is typically limited or prohibited altogether.

Construction and Operations Hazards

Most failures of cryogenic equipment can be traced to improper selection of construction materials or disregard for the change of some material property at low temperatures. For example, low temperatures make some construction materials brittle or less ductile. This behavior is further complicated because some materials become brittle at low temperatures but still can absorb considerable impact strength (see Chapter 40 for additional details). Brittle fracture can cause almost instantaneous failure, which can cause shrapnel damage if the system is under pressure, and release of a fluid such as oxygen can cause a fire or an explosion.

Low-temperature equipment can also fail because thermal stresses cause thermal contraction of the materials. Figure 44 provides information for evaluating the thermal contraction exhibited by several metals used widely in low-temperature construction. Solder in joints must be able to withstand stresses caused by differential contraction where two dissimilar metals are joined. Contraction in long pipes is also a serious problem; for example, a stainless steel pipeline 100 ft long will contract approximately 2.3 in. when filled with liquid oxygen or nitrogen. Provisions must be made for this change in length

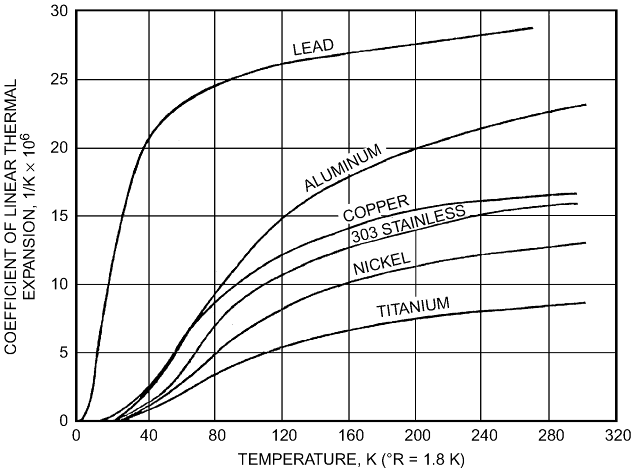

Fig. 44 Coefficient of Linear Expansion for Several Metals as Function of Temperature

during both cooling and warming of the pipeline by using bellows, expansion joints, or flexible hose. Pipe anchors, supports, and so on must also be carefully designed to allow contraction and expansion. The primary hazard of failure caused by thermal contraction is cryogen spillage and the possibility of fire or explosion.

Overpressure. All cryogenic systems should be protected against overpressure caused by phase change from liquid to gas. Systems containing liquid cryogens can reach bursting pressures, if not relieved, simply by trapping the liquid in an enclosure. Figure 45 shows the pressure build-up in a closed vessel of liquid nitrogen. The rate of pressure rise in storage containers for cryogens depends on the rate of heat transfer into the liquid. In uninsulated systems, liquid vaporizes rapidly and pressure in the closed system can rise very rapidly. The more liquid that is originally in the tank before it is sealed off, the greater will be the resulting final pressure.

Heat leakage and vaporization of cryogenic fluid trapped in valves, fittings, and sections of piping can cause excessive pressure buildup and possible rupture of the equipment. For instance, liquid hydrogen expands about 850 times its volume when warmed to ambient temperature. Relief valves and burst disks are normally used to relieve piping systems at a pressure slightly above the operating design pressure of the equipment. Relief should be provided between valves, on tanks, and at all locations of possible (though perhaps unintentional) pressure rise in a piping system.

Overpressure in cryogenic systems can also occur more subtly. Vent lines without appropriate rain traps can collect rainwater and freeze closed, as can exhaust tubes on relief valves and burst disks. Small-necked, open-mouth dewars can collect moisture from the air and freeze closed. Cold liquids or gases can be trapped by freezing water or other condensables in some portion of the cold system. If this occurs in an unanticipated location, the relief valve or burst disk may be isolated and afford no protection.

Another source of system overpressure that is frequently overlooked is cooldown surges. If a liquid cryogen is admitted to a warm line with the intention of transferring the liquid from one point to another, severe pressure surges will occur. These pressure surges can be 10 times the operating or transfer pressure and can even cause backflow into the storage container. The overall design and operating procedures for the transfer systems must protect against such overpressure.

Release of Cryogens. Although several cryogenic liquids produce vapors of lower molecular mass than air, the lower temperatures result in a denser vapor. Released vapors travel along the ground and collect in low places. Exposure to these vapors is hazardous. Exposure to oxygen vapors has caused clothing or any equipment with oil-lubricated parts to become oxygen-enriched and cause fires.

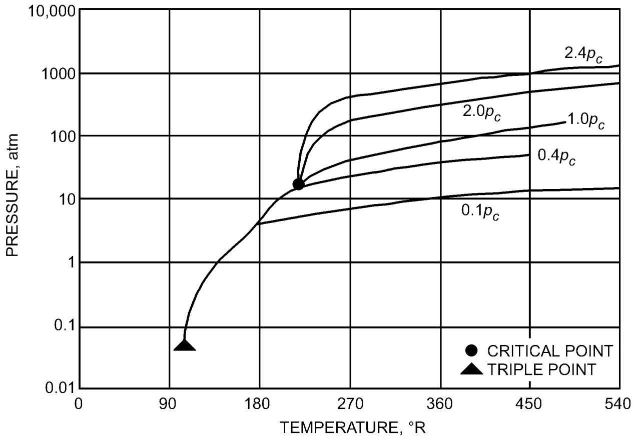

Fig. 45 Pressure Developed During Warming of Liquid Nitrogen in Closed Container

(Courtesy of Air Products and Chemicals, Inc., Allentown, PA)

In making an accident or safety analysis, the possibility of encountering even more serious secondary effects from any cryogenic accident should be considered. For example, any one of the failures discussed previously (brittle fracture, contraction, overpressure, etc.) may release sizable quantities of cryogenic liquids or cold gases, causing severe fire or explosion hazards, asphyxiation dangers, further brittle fracture problems, or shrapnel damage to other flammable or explosive materials. In this way the accident can rapidly and progressively become much more serious.

Flammability and Detonability Hazards

Almost any flammable mixture will, under favorable conditions of confinement, support an explosive flame propagation or even a detonation. A fuel/oxidant composition favorable for high-speed combustion first loses its capacity to detonate when it is diluted with an oxidant, fuel, or inert substance. Further dilution causes it to lose its capacity to burn explosively. Eventually, the lower or upper flammability limits will be reached and the mixture will not maintain its combustion temperature and will extinguish itself. These principles apply to the combustible cryogens, hydrogen and methane. The flammability and detonability limits for these two cryogens with either air or oxygen are presented in Table 9. Because the flammability limits are rather broad, great care must be exercised to exclude oxygen from these cryogens, particularly from hydrogen: even trace amounts of oxygen will condense, solidify, and build up with time in the bottom of the liquid hydrogen storage container, and eventually the upper flammability limits will be reached. Then some ignition source, such as a mechanical or electrostatic spark, may initiate a fire or possibly an explosion.

Liquid hydrogen and LNG spills form a vapor blanket that includes zones of combustible mixtures that could ignite the entire spilled fuel. Both these fluids burn clean; hydrogen produces a nearly invisible flame. Compared to a flammability limit of 2 to 9% (by volume) for jet fuel in air, hydrogen has a flammability limit of 4 to 75%, and LNG from 5 to 15%. The ignition of explosive mixtures of hydrogen with oxygen or air occurs with low energy input, about one-tenth that of a gasoline/air mixture. All ignition sources should be eliminated, and all equipment and connections should be grounded. Lightning protection (lightning rods, aerial cables, and ground rods suitably connected) should be provided at all preparation, storage, and use areas for these flammable cryogenic fluids.

The methane/oxygen/nitrogen flammability limits diagram of Figure 46 can be used to analyze a fuel/oxidant/diluent. The diagram is typical of any system where methane represents any fuel, oxygen represents any oxidant, and nitrogen represents any diluent. Gas mixtures that lie outside the flammability envelope will not burn or detonate because insufficient heat is released upon combustion to attain a temperature at which combustion is supported. Flame temperatures are at a minimum around the edges of the envelope but increase toward the center of the envelope. The line drawn from a 21% O_2/79% N_2 binary to pure CH_4 represents the compositions that can result from mixing methane with air. Flammability occurs from about 5 to 15% methane in air. If an LNG tank is

Table 9 Flammability and Detonability Limits of Hydrogen and Methane Gas

Mixture	Flammability Limits, mol %	Detonability Limits of Mixture, mol %
H_2/Air	4 to 75	20 to 65
H_2/O_2	4 to 95	15 to 90
CH_4/Air	5 to 15	6 to 14
CH_4/O_2	5 to 61	10 to 50

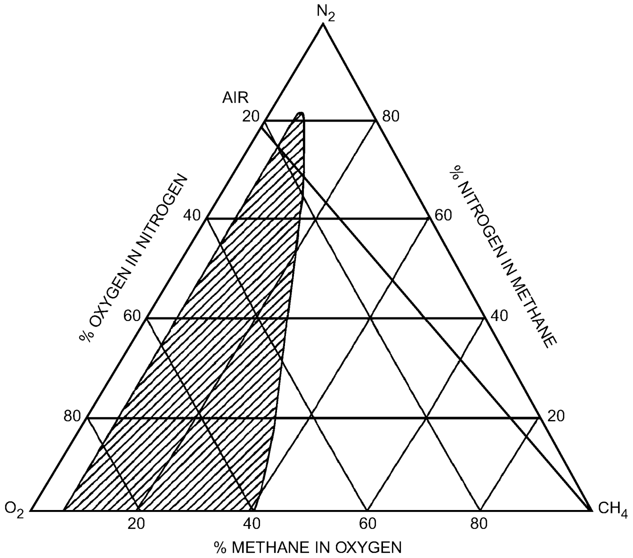

Fig. 46 Flammable Limits for $O_2/N_2/CH_4$ System
(Courtesy of Air Products and Chemicals, Inc., Allentown, PA)

purged with air, the resulting gas mixture would at first be too rich in methane for combustion. However, as purging continues, flammable mixtures would develop, resulting in a hazardous condition.

Such predictable behavior, however, depends on the homogeneous composition of the fuel/oxidant/diluent mixture achievable in gases. Where local concentration gradients exist, combustion behavior is less certain. In such cases, flame velocity depends on such factors as particle size, droplet size, and heat capacities of components in the system. Flame arresters, which are inserted in a line or vessel, prevent propagation of a flame front by absorbing energy from the combustion process and lowering the flame temperature below a level that supports combustion. The minimum ignition energy, however, varies considerably, being as much as an order of magnitude lower for a hydrogen/air mixture than for a methane/air mixture.

Flammable cryogens are best disposed of in a burnoff system in which the liquid or gas is piped to a remote area and burned with air in multiple burner arrangements. Such a system should include pilot ignition methods, flameout warning systems, and means for purging the vent line.

Because of its chemical activity, oxygen also presents a safety problem in handling. Liquid oxygen is chemically reactive with hydrocarbon materials. Ordinary hydrocarbon lubricants are even dangerous to use in oxygen compressors and vacuum pumps exhausting gaseous oxygen. In fact, valves, fittings, and lines used with oil-pumped gases should never be used with oxygen. Serious explosions have resulted from combining oxygen and hydrocarbon lubricants. To ensure against such unwanted chemical reactions, systems using liquid oxygen must be kept scrupulously clean of any foreign matter.

Liquid oxygen equipment must also be constructed of materials incapable of initiating or sustaining a reaction. Only a few polymeric materials can be used in such equipment, because most will react violently with oxygen under mechanical impact. Also, reactive metals such as titanium and aluminum should be used cautiously, because they are potentially hazardous. Once the reaction is started, an aluminum pipe containing oxygen burns rapidly and intensely. With proper design and care, however, liquid oxygen systems can be operated safely.

Although nitrogen is an inert gas and will not support combustion, in some subtle ways a flammable or explosive hazard may develop. Cold traps or open-mouth dewars containing liquid nitrogen can condense air and cause oxygen enrichment of the liquid nitrogen. The composition of air as it condenses into the liquid nitrogen container is about 50% oxygen and 50% nitrogen. As the liquid nitrogen evaporates, the liquid oxygen content steadily increases so that the last portion of liquid to evaporate will have a relatively high oxygen concentration. The nitrogen container must then be handled as if it contained liquid oxygen; fire, compatibility, and explosive hazards all apply to this oxygen-enriched liquid nitrogen.

Because air condenses at a temperature above the normal boiling point of liquid nitrogen, uninsulated pipelines transferring liquid nitrogen will condense air. This oxygen-enriched condensate can drip on combustible materials, causing an extreme fire hazard or explosive situation. The oxygen-rich condensate can saturate clothing, rags, wood, asphalt pavement, etc., and cause the same problems associated with the handling and spillage of liquid oxygen.

Hazard Evaluation Summary

The best-designed facility is no better than the detailed attention paid to every aspect of safety. Such attention cannot be considered once and forgotten. Rather, it is an ongoing activity that requires constant review of every conceivable hazard that might be encountered.

REFERENCES

Alexeev, A., C. Haberstroh, and H. Quack. 1999. Mixed gas J-T cryocooler with precooling stage. *Cryocoolers*, vol. 10, R.G. Ross, Jr., ed. Kluwer Academic/Plenum Publishers.

Alfiev, V.N., V.M. Brodyansky, V.M. Yagodin, V.A. Nikolsky, and A.V. Invantso. 1973. *Refrigerant for a cryogenic throttling unit*. U.K. Patent 1,336,892.

ASME. 2004. *Boiler and pressure vessel code.* American Society of Mechanical Engineers, New York.

ASTM. 2004. Standard practice for estimate of the heat gain or loss and the surface temperatures of insulated flat, cylindrical, and spherical systems by use of computer programs. *Standard* C680-04e1. American Society for Testing and Materials, West Conshohocken, PA.

ASTM. 2001. Standard practice for calculating thermal transmission properties under steady-state conditions. *Standard* C1045-01. American Society for Testing and Materials, West Conshohocken, PA.

Arp, V. 1997. Electrical and thermal conductivities of elemental metals below 300 K. *Proceedings of the 13th Symposium on Thermophysical Properties*, Boulder, CO.

Arp, V. 1998. A summary of fluid properties including near-critical behavior. *Proceedings of the International Conference on Cryogenics and Refrigeration*, Hangzhou, China.

Barron, R.F. 1985. *Cryogenic systems*, 2nd ed. Oxford University Press, London.

Bednorz, J.G. and K.A. Müller. 1986. Possible high superconductivity in the Ba-La-Cu-O system. *Zeitschrift für Physik B* (now *European Physical Journal*) 64(2):189-193.

Broerman, E., et al. 2001. Performance of a new type of electrical cooler for HPGe detector systems. Institute of Nuclear Materials Management Conference, India Head, CA.

Burt, W.W. and C.K. Chan. 1995. Demonstration of a high performance 35 K pulse-tube cryocooler. *Cryocoolers 8*, p. 313. Plenum Press, New York.

Davey, G. 1990. Review of the Oxford cryocooler. *Advances in Cryogenic Engineering*, vol. 35, p. 1423. Plenum Press, New York.

Dobak, J.D., R. Radebaugh, M.L. Huber, and E.D. Marquardt. 1998. *Mixed gas refrigerant method*. U.S. Patent 5,787,715.

Eckels Engineering. 2003. *CRYOCOMP*, v. 2.0. Available at http://www.htess.com/cryocomp.htm.

Gaumer, L.S. 1986. LNG processes. *Advances in Cryogenic Engineering*, vol. 31, p. 1095. Plenum Press, New York.

Grenier, M. and P. Petit. 1986. Cryogenic air separation: The last twenty years. *Advances in Cryogenic Engineering*, vol. 31, p. 1063. Plenum Press, New York.

Hashimoto, T., M. Ogawa, A. Hayaski, M. Makino, R. Li, and K. Aoki. 1992. Recent progress on rare earth magnetic regenerator materials. *Advances in Cryogenic Engineering*, vol. 37, p. 859. Plenum Press, New York.

Keppler, F., G. Nellis, and S.A. Klein. 2004. Optimization of the composition of a gas mixture in a Joule-Thomson cycle. *International Journal of HVAC&R Research* 10(2):213-230.

Kleemenko, A.P. 1959. One flow cascade cycle. *Proceedings of the Xth International Congress of Refrigeration*, Copenhagen, vol. 1, pp. 34-39. Pergamon Press, London.

Klein, S.A. Continuously updated. *EES—Engineering equation solver.* F-Chart Software, Madison, WI. (fchart.com)

Kuriyama, T., M. Takahashi, H. Nakagoma, T. Hashimoto, H. Nitta, and M. Yabuki. 1994. Development of 1 watt class 4K GM refrigerator with magnetic regenerator materials. *Advances in Cryogenic Engineering*, vol. 39, p. 1335. Plenum Press, New York.

Little, W.A. 1984. Microminiature refrigeration. *Review of Scientific Instruments* 55:661-680.

Little, W.A. 1990. Advances in Joule Thomson cooling. *Advances in Cryogenic Engineering*, vol. 35, p. 1305. Plenum Press, New York.

Little, W.A. 1997a. *Self-cleaning low-temperature refrigeration system.* U.S. Patent 5,617,739.

Little, W.A. 1997b. *Method for efficient counter current heat exchange using optimized mixtures.* U.S. Patent 5,644,502.

Little, W.A. 1998. Kleemenko cycle coolers: Low cost refrigeration at cryogenic temperatures. ICEC 17, Bournemouth, U.K. Institute of Physics Publishing, Bristol and Philadelphia.

Little, W.A. 2003. Seven year history of continuous operation of Kleemenko cryocoolers. M-CALC IV, Strategic Analysis, Inc.

Little, W.A. and I. Sapozhnikov. 1998. *Self-cleaning cryogenic refrigeration system*. U.S. Patent 5,724,832.

Longsworth, R.C. 1997a. *Cryogenic refrigerator with single stage compressor.* U.S. Patent 5,337,572.

Longsworth, R.C. 1997b. 80 K throttle-cycle refrigerator cost reduction. *Cryocoolers 9*, R.G. Ross, Jr., ed. Plenum Press, New York.

M-CALC-IV. 2003. Fourth workshop on military and commercial applications of low-cost cryocoolers, November 20-21, 2003, Hyatt Islandia, San Diego, CA. Strategic Analysis, Inc. (www.sainc.com/MCALC4)

Missimer, D. J. 1973. *Self-balancing low temperature refrigeration system.* U.S. Patent 3,768,273.

Nagao, M., T. Anaguchi, H. Yoshimura, S. Nakamura, T. Yamada, T. Matsumoto, S. Nakagawa, K. Moutsu, and T. Watanabe. 1994. 4 K three stage Gifford-McMahon cycle refrigerator for MRI magnet. *Advances in Cryogenic Engineering*, vol. 39, p. 1327. Plenum Press, New York.

NIST. 2002a. *NIST standard reference database* 4, *SUPERTRAPP.* National Institute of Standards and Technology, Gaithersburg, MD.

NIST. 2002b. *NIST standard reference database* 14, *DDMAX*. National Institute of Standards and Technology, Gaithersburg, MD.

Radebaugh, R. 1990. A review of pulse tube refrigeration. *Advances in Cryogenic Engineering*, vol. 35, p. 1191. Plenum Press, New York.

Radebaugh, R. 1995. Recent developments in cryocoolers. *Proceedings of the XIX International Congress of Refrigeration* IIIb:973. IIR, Paris.

Strobridge, T.R. 1974. Cryogenic refrigerators—An updated survey. NBS *Technical Note* 655. National Bureau of Standards, U.S. Government Printing Office, Washington, D.C.

Swift, W.L. and H. Sixsmith. 1993. Performance of a long life reverse Brayton cryocooler. *Proceedings of the 7th International Cryocooler Conference*, vol. 84. Air Force *Report* PL CP 93 1001.

Wigley, D.A. 1971. *Mechanical properties of materials at low temperatures*. Plenum Press, New York.

Zhu, S., P. Wu, and Z. Chen. 1990. Double inlet pulse tube refrigerators: An important improvement. *Cryogenics* 30:514.

BIBLIOGRAPHY

Anderson, J.E., D.A. Fester, and A.M. Czysz. 1990. Evaluation of long term cryogenic storage system requirements. *Advances in Cryogenic Engineering*, vol. 35, p. 1725. Plenum Press, New York.

Augustynowicz, S.D., J.A. Demko, and V.I. Datskov. 1994. Analysis of multilayer insulation between 80 K and 300 K. *Advances in Cryogenic Engineering*, vol. 39, p. 1675. Plenum Press, New York.

Edeskuty, F.J. and W.F. Stewart. 1986. *Safety in the handling of cryogenic fluids*. Plenum Press, New York.

Edeskuty, F.J. and K.D. Williamson. 1983. *Liquid cryogens*, vols. 1 and 2. CRC Press, Boca Raton, FL.

Gistan, G.M., J.C. Villard, and F. Turcat. 1990. Application range of centrifugal compressors. *Advances in Cryogenic Engineering*, vol. 35, p. 1031. Plenum Press, New York.

Hashimoto, T., K. Gang, H. Makuuchi, R. Li, A. Oniski, and Y. Kanazawa. 1994. Improvement of refrigeration characteristics of the G-M refrigerator using new magnetic regenerator material ErNi$_{1-x}$CO$_x$ system. *Advances in Cryogenic Engineering*, vol. 37, p. 859. Plenum Press, New York.

Haynes, W.M. and D.G. Friend. 1994. Reference data for thermophysical properties of cryogenic fluids. *Advances in Cryogenic Engineering*, vol. 39, p. 1865. Plenum Press, New York.

Jacobsen, R.T. and S.G. Penoncello. 1997. *Thermodynamic properties of cryogenic fluids*. Plenum Press, New York.

Johnson, P.C. 1986. Updating LNG plants. *Advances in Cryogenic Engineering*, vol. 31, p. 1101. Plenum Press, New York.

Kittel, P. 1992. Ideal orifice pulse tube refrigerator performance. *Cryogenics* 32:843.

Kun, L.C. 1988. Expansion turbines and refrigeration for gas separation and liquefaction. *Advances in Cryogenic Engineering*, vol. 33, p. 963. Plenum Press, New York.

Lee, J.M., P. Kittel, K.D. Timmerhaus, and R. Radebaugh. 1993. Flow patterns intrinsic to the pulse tube refrigerator. *Proceedings of the 7th International Cryocooler Conference*, p. 125. Air Force *Report* PL CP 93 1001.

Lemmon, E.W., R.T. Jacobsen, S.G. Penoncello, and S.W. Beyerlein. 1994. Computer programs for the calculation of thermodynamic properties of cryogens and other fluids. *Advances in Cryogenic Engineering*, vol. 39, p. 1891. Plenum Press, New York.

Longsworth, R.C. 1988. 4 K Gifford-McMahon/Joule-Thomson cycle refrigerators. *Advances in Cryogenic Engineering*, vol. 33, p. 689. Plenum Press, New York.

Pavese, F. and G. Molinas. 1992. *Modern gas-based temperature and pressure measurements*. Plenum Press, New York.

Rao, M.G. and R.G. Scurlock. 1986. Cryogenic instrumentation with cold electronics: A review. *Advances in Cryogenic Engineering*, vol. 31, p. 1211. Plenum Press, New York.

Sarwinski, R.E. 1988. Cryogenic requirements for medical instrumentation. *Advances in Cryogenic Engineering*, vol. 33, p. 87. Plenum Press, New York.

Scurlock, R.G. 1992. A brief history of cryogenics. *Advances in Cryogenic Engineering*, vol. 37, p. 1. Plenum Press, New York.

Shuh, Q.S., R.W. Fast, and H.L. Hart. 1988. Theory and technique for reducing the effect of cracks in multilayer insulation from room temperature to 77 K. *Advances in Cryogenic Engineering*, vol. 33, p. 291. Plenum Press, New York.

Sixsmith, H., R. Hasenbein, J.A. Valenzuela, J.C. Theilacker, and J. Fuerst. 1990. A miniature wet turboexpander. *Advances in Cryogenic Engineering*, vol. 35, p. 989. Plenum Press, New York.

Spradley, I.E., T.C. Nast, and D.J. Frank. 1990. Experimental studies of MLI systems at very low boundary temperatures. *Advances in Cryogenic Engineering*, vol. 35, p. 477. Plenum Press, New York.

Storch, P.J. and R. Radebaugh. 1988. Development and experimental test of an analytical model of the orifice pulse tube refrigerator. *Advances in Cryogenic Refrigeration* 33:851-859.

Timmerhaus, K.D. and T.M. Flynn. 1989. *Cryogenic process engineering*. Plenum Press, New York.

Van Sciver, S.W. 1991. *Helium cryogenics*. Plenum Press, New York.

Vinen, W.F. 1990. Fifty years of superfluid helium. *Advances in Cryogenic Engineering*, vol. 35, p. 1. Plenum Press, New York.

Walker, G. 1983. *Cryocoolers*. Plenum Press, New York.